MICROFILTRATION WITH RAPID BACKPULSING AND SURFACE-MODIFIED MEMBRANES

Robert H. Davis and Christopher N. Bowman
Department of Chemical Engineering
University of Colorado
Boulder, CO 80309-0424

Contract No. 1425-98-FC-81-0062

Desalination Research and Development Program Report No. 58

December 1999

U.S. DEPARTMENT OF THE INTERIOR
Bureau of Reclamation
Denver Office
Technical Service Center
Environmental Resources Team
Water Treatment Engineering and Research Group

Bureau of Reclamation Mission Statement

The mission of the Bureau of Reclamation is to manage, develop, and protect water and related resources in an environmentally and economically sound manner in the interest of the American public.

U. S. Department of the Interior Mission Statement

As the Nation's principal conservation agency, the Department of the Interior has responsibility for most of our nationally-owned public lands and natural resources. This includes fostering wise use of our land and water resources; protecting our fish, wildlife, and biological diversity; preserving the environmental and cultural values of our national parks and historical places; and providing for the enjoyment of life through outdoor recreation. The Department assesses our energy and mineral resources and works to ensure that their development is in the best interests of all our people by encouraging stewardship and citizen participation in their care. The Department also has a major responsibility for American Indian reservation communities and for people who live in island territories under U.S. Administration.

Disclaimer

The information contained in this report regarding commercial products or firms may not be used for advertising or promotional purposes and is not to be construed as an endorsement of any product or firm by the Bureau of Reclamation.

The information contained in this report was developed for the Bureau of Reclamation: no warranty as to the accuracy, usefulness, or completeness is expressed or implied.

TABLE OF CONTENTS

	Page
EXECUTIVE SUMMARY	1
1. INTRODUCTION	1
2. MATERIALS AND METHODS	4
2.1 Membrane Surface Modification	4
2.2 Crossflow Filtration	5
3. RESULTS AND DISCUSSION	6
3.1 Photografting on Membrane Surfaces	6
3.2 Membrane Performance	15
3.3 Fundamental Analysis of Membrane Fouling	21
3.4 Economic Analysis and Comparisons	22
4. CONCLUSIONS	24
REFERENCE LIST	25
APPENDIX: DATA RECORD	28

LIST OF FIGURES

Figure 1. Schematic diagram of the two-step photoinduced living graft polymerization method 3

Figure 2. Schematic diagram of the crossflow filtration system 6

Figure 3. Grafting density versus irradiation time at different BP concentrations 8

Figure 4. Average graft polymer chain length versus irradiation time at different AA concentrations 9

Figure 5. Reaction rates of initiator formation versus BP concentrations 11

Figure 6. Reaction rates of graft polymerization versus AA concentration 12

Figure 7. Amount of surface initiator vs. BP concentration 13

Figure 8. Weight gain as a function of AA concentration for graft polymerization on CA membranes 14

Figure 9. Pure buffer flux at 5 psi versus the amount of grafted PEG200MA 16

Figure 10. Permeate flux versus filtration time of 0.14 g/L *E. coli* without backpulsing at a forward transmembrane pressure of 5 psi 16

Figure 11. Average neg flux (symbols) versus backpulse duration for crossflow filtration of 0.14 g/L *E. coli* at a forward filtration time of 4 seconds between backpulses, with forward transmembrane pressure of 5 psi and backward transmembrane pressure of 3 psi 17

Figure 12. Average net flux (symbols) versus forward filtration duration for crossflow filtration of 0.14 g/L *E. coli* at a fixed backpulse duration of 0.2 seconds, with forward transmembrane pressure of 5 psi and backward transmembrane pressure of 3 psi 17

Figure 13. Permeate volume verses filtration time for crossflow filtration of 0.14 g/L *E. coli*.. 18

Figure 14. Long-term net flux with backpulsing and recovered flux after backwashing versus the amount of grafted PEG200MA for crossflow filtration of 0.14 g/L *E. coli* 20

Figure 15: Schematic of partial cake removal by backpulsing 21

Figure 16: Experimental data and model prediction of the net flux versus the duration of each backpulse for crossflow microfiltration of 1.0 g/L *E. coli* bacteria using 0.2 μm cellulose-acetate membranes and a forward filtration period of 10 s between each backpulse 22

Figure 17. Total cost of treated water as a function of the average net permeate flux for 0.5 MGD and 10 MGD membrane treatment facilities 23

LIST OF TABLES

Table 1. Weight percent gain of PP membranes and standard deviation for six repeats in air or nitrogen 7

Table 2. Weight percent gain of PP membranes and standard deviation for six repeats 7

Table 3. Properties of Polymeric Membranes in Two-Step Graft Polymerization 14

Table 4. Effect of membrane surface chemistry on long-term flux and recovered flux after backwashing, with and without backpulsing. Shown are the average plus and minus one standard deviation for 2-6 repeats 19

Table 5. Effects of *E. coli* concentration on the average net flux with backpulsing, long-term net flux with backpulsing and recovered flux after backwashing for unmodified PP membranes and modified PP membranes with a weight gain of 3.5 wt% PEG200MA. Shown are the averages plus and minus one standard deviation for 2-4 repeats 21

Table 6. Long-term net flux and treatment cost for removal of 0.05 g/L bacteria from water by crossflow membrane microfiltration using unmodified and modified polypropylene membranes with and without backpulsing. PEG200MA with 3.5 wt% gain was used for the membrane surface modification 24

ACRONYMS AND NOMENCLATURE

AA	- acrylic acid (monomer)
AF	- amortization factor
BP	- benzophenone (initiator)
BPHS	- surface initiator
C_{mod}	- the cost of single membrane module
CA	- cellulose acetate (membrane)
D	- grafting density
DMAEMA	- dimethyl aminoethyl methacrylate (monomer)
f	- surface initiator formation efficiency
G_e	- grafting efficiency
I_0	- intensity of UV irradiation
$\langle J \rangle$	- net flux with backpulsing (cm/s)
J_o	- water flux for unfouled membrane (cm/s)
J_s	- long-term flux for unfouled membrane (cm/s)
k_p	- propagation rate constant
k_t	- termination rate constant
N_{mod}	- the number of modules required
PEG200MA	- polyethylene glycol (200) monomethacrylate (monomer)
PP	- polypropylene (membrane)
PVDF	- poly(vinylidene fluoride) (membrane)
Q	- volumetric treatment rate
R_m	- rate of monomer consumption
t_b	- backpulse duration (s)
t_f	- duration of forward filtration between backpulses (s)
UV	- ultraviolet
α	- ratio of backpulse and forward transmembrane pressures
β	- cleaning efficiency
γ	- graft polymer chain length
ϕ	- quantum yield of polymer formation
ϕ_s	- quantum yield of surface initiator formation
τ_b	- the time constant for cake removal

EXECUTIVE SUMMARY

A combined method of backpulsing and membrane surface modification was used for the reduction of membrane fouling in water-treatment applications. A novel photoinduced grafting method was used to render membranes hydrophilic with neutral, positively or negatively charged surfaces formed by grafting monomers of poly(ethylene glycol 200) monomethacrylate (PEG200MA), dimethyl aminoethyl methacrylate (DMAEMA), or acrylic acid (AA), respectively, onto a variety of substrates, including polypropylene (PP) and cellulose acetate (CA). Both unmodified and modified PP membranes, as well as commercial CA membranes, were evaluated in a crossflow microfiltration system with and without backpulsing in the presence of *Escherichia coli* bacterial suspensions. The grafting process on the surfaces studied was found to be controllable and reproducible. The process was modeled successfully and can be used to graft a variety of monomers with independent control of the graft density, chain length, and total amount.

For membrane studies it was found that without backpulsing the resulting permeate volume is nearly unchanged for a variety of different membranes. With backpulsing, however, the permeate volume for one hour of filtration with 0.14 g/L *E. coli* using the unmodified PP membranes is almost two times that without backpulsing, and it is significantly higher for the modified membranes. The optimal membrane process was found to be one which involved both backpulsing and modification with a neutral, hydrophilic surface graft. The permeate volume for such a PP membrane is almost three times that of the base case. Additionally, after cleaning, the recovered clean water flux of the modified membranes is twice as high as those for the unmodified membranes and even more improved when compared to unmodified membranes with backpulsing.

1. INTRODUCTION

Membrane systems have recently received increased attention for water treatment and other applications. However, a major obstacle to further incorporation of membrane processes in industrial operations is flux decline resulting from fouling. Membrane replacement, required because of fouling, is the single largest operating cost when membranes are used in water treatment applications (Wiesner et al., 1994). Generally, two distinct types of fouling phenomena are considered (Zeman and Zydney, 1996): (1) macrosolute adsorption, which refers to the specific intermolecular interactions between the macrosolute and the membrane that occur even in the absence of filtration, and (2) filtration-induced macrosolute or particle deposition, which is over and above that observed in a static (nonflowing) system.

Filtration-induced macrosolute or particle deposition is usually reversible, nonadhesive fouling. A variety of methods has been reported to reduce this type of fouling for a wide range of different applications:

(1) addition of coagulants to cause the molecules or the particle to form larger particles which are readily swept off the membrane surface (Al-Malack and Anderson, 1996),

(2) use of a dispersed phase to disrupt concentration polarization (Parvatiyar, 1996),

(3) introduction of flow instability by low-frequency axial pressure and velocity pulsing (Si-Hassen et al., 1996; Zahka and Leary, 1985), or by injecting air into the feed stream (Cabassud et al., 1997),

(4) crossflushing by periodically stopping the permeate flow (Kuruzovich and Piergiovanni, 1996) or forward rinsing with a rinse solution at zero transmembrane pressure (Nakanishi and Kessler, 1985),

(5) backwashing using fluid or gas (Kroner et al., 1984; Nikolov et al., 1993),

(6) forward and backward pressure pulsing to remove part of the adsorbed cake (Su et al., 1993),

(7) imposing a pulsed electric field to remove particulate foulants when the membrane and particles have like charges (Bowen and Sabuni , 1992),

(8) using curved channel to produce Taylor or Dean vortices (Parnham and Davis, 1995; Chung et al., 1993), and

(9) rapid backpulsing (Rodgers and Sparks, 1991, 1992, 1993; Wenton, 1995; Redkar and Davis, 1995).

As described by Kuberkar et al. (1998), rapid backpulsing in crossflow filtration involves reversing the transmembrane pressure for approximately 0.1-1.0 second once every few seconds. This reversal results in hydraulic cleaning of the membrane by forcing permeate back through the membrane in the reverse direction; foulants are lifted off the membrane by the backpulse and then swept to the filter exit by the crossflow. Crossflow filtration with rapid backpulsing has been studied extensively by a number of groups in various membrane/foulant systems, and has been reported as an effective technology for controlling fouling and improving permeate flux for nonadhesive foulants exhibiting reversible fouling (Rodgers and Sparks, 1993; Wenton, 1995; Redkar and Davis, 1995). Unfortunately, rapid backpulsing is much less effective in reducing adhesive fouling (Kroner et al., 1984; Kuberkar et al., 1998; Parnham and Davis, 1996).

Macrosolute adsorption is generally irreversible, adhesive fouling (Zeman and Zydney (1996). In water treatment applications involving colloids, microbes, and undissolved hydrocarbons, the foulants are often adhesive and exhibit irreversible fouling, due to hydrophobic interactions, ionic interactions, hydrogen bonding, van der Waals attractions, extracellular macromolecules, and other effects. Several methods have been reported for reducing or eliminating adhesive fouling by changing the membrane surface chemistry. These methods include: (1) physically coating water soluble polymers or charged surfactants onto the membrane surface for temporary surface modification (Kim et al., 1988; Jonsson and Jonsson, 1991), (2) forming ultrathin films on the membrane using the Langmuir-Blodgett (LB) technique (Kim et al., 1989), (3) coating hydrophilic polymers on the membrane using heat curing (Stengaard, 1988; Hvid et al., 1990), (4) grafting monomers to the membranes by electron beam irradiation (Kim et al., 1991; Keszler et al., 1991), and (5) photografting monomers to the membrane using UV irradiation (Yan et al., 1988; Nystrom and Jarvinen, 1991; Yamagishi et al., 1995; Ulbricht et al., 1996).

Photoinduced grafting is a particularly useful technique for the modification and functionalization of polymeric materials due to its significant advantages: low cost of operation, mild reaction conditions, selectivity to absorb UV light without affecting the bulk polymer, and permanent alteration of the membrane surface with facile control of the chemistry. Several researchers (Ulbricht et al., 1996; Yamagishi et al., 1995) have reported the reduction of irreversible protein (BSA) fouling when membrane surfaces are modified by photografting. However, simultaneous photografting (with photoinitiator and monomer present together) may result in production of significant amounts of homopolymer and crosslinked polymer, for cases where the photoinitiator abstracts hydrogen from either the monomer or reacted polymer. The undesired homopolymer wastes expensive starting materials, and crosslinked polymer is detrimental to membrane filtration since the membrane pores may become blocked. Moreover, the grafting density (number of grafting sites per area) and graft polymer chain length can not be determined independently, much less controlled, in the previously developed process.

A novel photografting technique was designed and developed as part of this work and is currently awaiting publication in *Macromolecules* (Ma et al., 1999). With this technique, homopolymer and crosslinked polymer can be significantly reduced, linear polymer chains are preferred, and the grafting density and graft polymer chain length are controlled independently. The schematic reaction mechanism for the grafting reaction is shown in Figure 1. In the first step, benzophenone abstracts hydrogen from the substrate to generate surface radicals and semipinacol radicals, which combine to form surface photoinitiators in the absence of monomer solutions. The unreacted benzophenone is then washed off by a good solvent. In the subsequent step(s), the monomer solutions are added onto the active substrate, and the surface initiators initiate the graft polymerization upon exposure to UV irradiation. Both homopolymer and crosslinked polymer are reduced in the novel grafting method, since benzophenone is not present at the same time with monomer or grafted polymer.

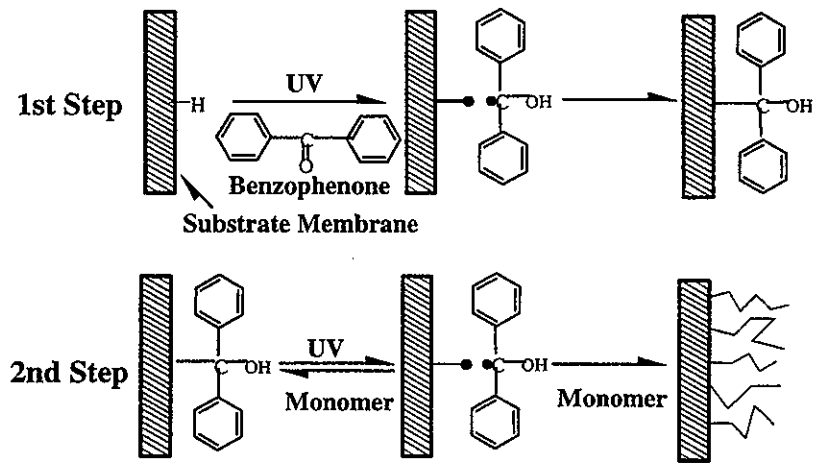

Figure 1. Schematic diagram of the two-step photoinduced living graft polymerization method.

Both reversible and irreversible fouling are reduced by the combination of backpulsing and membrane surface modification as demonstrated by the following results. Results are presented for detailed studies on the grafting reaction, modeling of the grafting, and evaluation of membrane performance for both modified and unmodified membranes. Both unmodified and modified PP membranes, as well as commercial cellulose acetate (CA) membranes, were tested in a crossflow microfiltration system with and without backpulsing in the presence of *Escherichia coli* bacterial suspensions.

In the first study of fouling reduction in wastewater treatment funded by the Bureau of Reclamation, it was found that rapid backpulsing was quite effective in maintaining high permeate fluxes when treating suspensions of nonadhesive matter. However, for highly adhesive foulant suspensions, rapid backpulsing is much less effective in reducing membrane fouling. Therefore, in the second study of the subject, a combined method of rapid backpulsing and membrane surface modification was proposed to reduce both nonadhesive and adhesive fouling. The original objectives of the project were met, and an extra effort was required for developing a novel grafting method to modify membrane surface chemistry. In the current study of the subject, the novel photografting method was investigated using commercial photopolymerization equipment. The membrane surface chemistry, grafting density, and graft chain length were well controlled. Most of the fouling characterization and backpulsing studies were performed with the modified polypropylene membranes, and the interactions between foulant and membrane surface were examined.

2. MATERIALS AND METHODS

2.1. Membrane Surface Modification

The base membranes used in the experiments are commercial porous disk polypropylene microfiltration membranes with a diameter of 47 mm, thickness of approximately 110 μm, porosity of 40 %, and pore diameter of 0.22 μm (Micron Separations Inc., M02WP04700), and cellulose acetate microfiltration membranes with a diameter of 47 mm, thickness of approximately 120 μm, and pore diameter of 0.22 μm (Sartorius, Cat. 11127-047N). Acrylic acid (AA) (Aldrich, cat. 14,723-0), poly(ethylene glycol 200) monomethacrylate (PEG200MA) (Polyscience, Inc., cat. 16712), and dimethyl aminoethyl methacrylate (DMAEMA) (Aldrich, cat. 23,490-7) were used as the monomers. All three monomers are hydrophilic. AA is negatively charged, DMAEMA is positively charged, and PEG200MA is neutral. Unmodified PP and CA membranes are hydrophobic and hydrophilic, respectively, and they are both neutral. Benzophenone (BP) (Aldrich, Cat. No. B930-0) was used as the initiator. Benzene, acetone, and deionized water were used as solvents. All chemicals were used without purification.

Both sequential and simultaneous photoinduced graft polymerization methods were used in the present work. First, the commercial PP membranes were soaked in benzene and dried to constant weight. Then, the membranes were weighed using an analytical balance which has an accuracy of 0.01 mg. For the sequential method, in the first step, the presoaked and preweighed membranes were saturated with benzene solutions of BP (3 g of solution was added to the membrane) and then placed in a quartz reaction vessel, which was subsequently purged with nitrogen or air. The quartz vessel is an empty cylinder with a diameter of 25 cm and a height of 2.5 cm. UV irradiation was carried out in a commercial ultraviolet processor (model QC120244ANIRDR, manufactured by RPC Industries), which was donated by 3M. The processor is equipped with 2 UV bulbs; each bulb is 400 W with a wavelength range of 232 nm to 500 nm. An optical multi-layer dielectric interference filter (365 ± 5 nm), from Edmund Scientific (Stock No. F43155), was used in the kinetic experiments. The quartz vessel was put on the conveyor, which carried the quartz vessel under the UV lamps. After irradiation for a selected number of passes, the substrates were removed from the quartz vessel, and the residual, unreacted solutions were extracted by soaking and washing the membrane in acetone and drying the membrane at room temperature in air until constant weight. In the subsequent step, the procedures in the first step were repeated, except that monomer solutions were used instead of BP solutions and that the membrane was put in a vacuum oven at 127 mm Hg and 50 °C to evaporate the residual, unreacted solutions. The nongrafted poly(acrylic acid) was removed by soaking the membranes in deionized water for 24 hours. Finally, the membranes were washed in acetone and dried to constant weight. For the simultaneous method, the procedures are similar to the procedures of the second step in the sequential method, except that both BP and monomer are present in the benzene solution.

The percent graft of BP, percent graft of monomer, grafting density, graft polymer chain length, and grafting efficiency are calculated by the following formulae:

$$\text{Percent graft of BP} = (W_1-W_0)/W_0\times 100\%, \quad (1)$$

$$\text{Percent graft of monomer} = (W_2 - W_1)/W_0\times 100\%, \quad (2)$$

$$\text{Grafting density, } D = (W_1-W_0)/MW_{BP}/V, \quad (3)$$

$$\text{Graft polymer length, } \gamma = [(W_2 - W_1)/MW]/[(W_1-W_0)/MW_{BP}], \quad (4)$$

$$\text{Grafting efficiency, } G_E = (W_2 - W_1)/(W_3-W_0)*100\%, \quad (5)$$

where W_0 is the weight of the blank membrane, W_1 is the weight of the membrane after the first step, obtained by weighing after extraction of unreacted BP solutions with proper solvents, W_2 is the weight of the membrane after the second step, obtained by weighing after extraction of

homopolymer with proper solvents, V is the volume of the membrane pores, MW_{BP} and MW are the molecular weight of BP and monomer, respectively, and W_3 is the weight of the membrane with both ungrafted and grafted polymer, obtained by weighing after vaporization of residual monomer and solvent solutions. The weight gain measurements were made using an analytical balance (Denver Instrument Company, A-200DS), which has an accuracy of 0.01 mg.

2.2. Crossflow Filtration

The original *E. coli* strain RB791 sample was obtained from the lab of Dr. George Georgiou at the University of Texas, Austin. Subsequent cultures were grown for 24 hours in a shaker water bath at 37°C and 200 rpm using M9 medium (Sambrook et al., 1989) and then centrifuged using a Beckman GPR Centrifuge at 2500 rpm for 30 minutes. Dry cell weights of 0.05-0.6 g/L *E. coli* resuspended in a buffer solution were used for the microfiltration experiments. The *E. coli* concentration was measured using a Diode Array Spectrophotometer (Hewlett 8452A). The buffer solution consists of 80 g NaCl, 14.4 g $NaHPO_4$, 2.4 g KH_2PO_4, and 2.0 g KCl in 10 liters of deionized water. All of these chemicals were obtained from Fisher Scientific. The *E. coli* cells are approximately 2 μm long and 0.5 μm wide.

A schematic diagram of the crossflow microfiltration system is shown in Figure 2. The feed flows from the pressurized feed tank to the crossflow module, which was fabricated in our instrument shop. A disk membrane with a diameter of 47 mm is used. The filtration area is 30 mm wide by 23 mm long, and the thickness of silicon gaskets between the membrane and the top plate of the module is 0.4 mm. The retentate flows from the module back to the feed tank. To keep the suspension concentration constant, buffer is pumped from a second tank to the feed tank at the rate at which permeate is removed. The permeate flows to a computer-interfaced balance which records the mass. During backpulsing, buffer from a third tank is sent through permeate channel up through the membrane in the direction opposite that of forward flow. The entire system is pressurized using a nitrogen tank. A QuickBasic program is used to monitor the solenoid valves, control the rate of fluid flow from the second tank to the feed tank, and record the balance readings. The program is run on a Data Stor 386-20D computer.

All experiments were run at room temperature (22-25°C). The PP membrane was wetted using ethanol just before each filtration experiment. The pure buffer flux was determined with plain buffer at a forward transmembrane pressure of 5 psi for five minutes. Then, *E. coli* filtration with or without backpulsing was performed for one hour. A new membrane was used for each experiment. For crossflow filtration with backpulsing, the forward transmembrane pressure was 5 psi and the backward transmembrane pressure was 3 psi. The specified duration of each backpulse was 0.1-0.5 seconds, and the forward filtration between each backpulse was for a specified duration of 2-14 seconds. After obtaining the average net flux (over the one-hour filtration period) and the long-term net flux (over the last 5 minutes of filtration, during which the flux remained steady), the backpulsing was stopped and the system was immediately backwashed for at least five minutes (which we found sufficient to remove all reversible foulants) at a reverse transmembrane pressure of 3 psi while still running buffer over the membrane. Finally, plain buffer was run through the membrane at 5 psi forward transmembrane pressure for five minutes to determine the recovered permeate flux.

For crossflow filtration without backpulsing, forward filtration was performed at a transmembrane pressure of 5 psi for one hour. The long-term flux was determined over the last five minutes in the filtration process (during which the flux remained steady). The backwashing process and recovered flux measurements were performed in the same way as those with backpulsing.

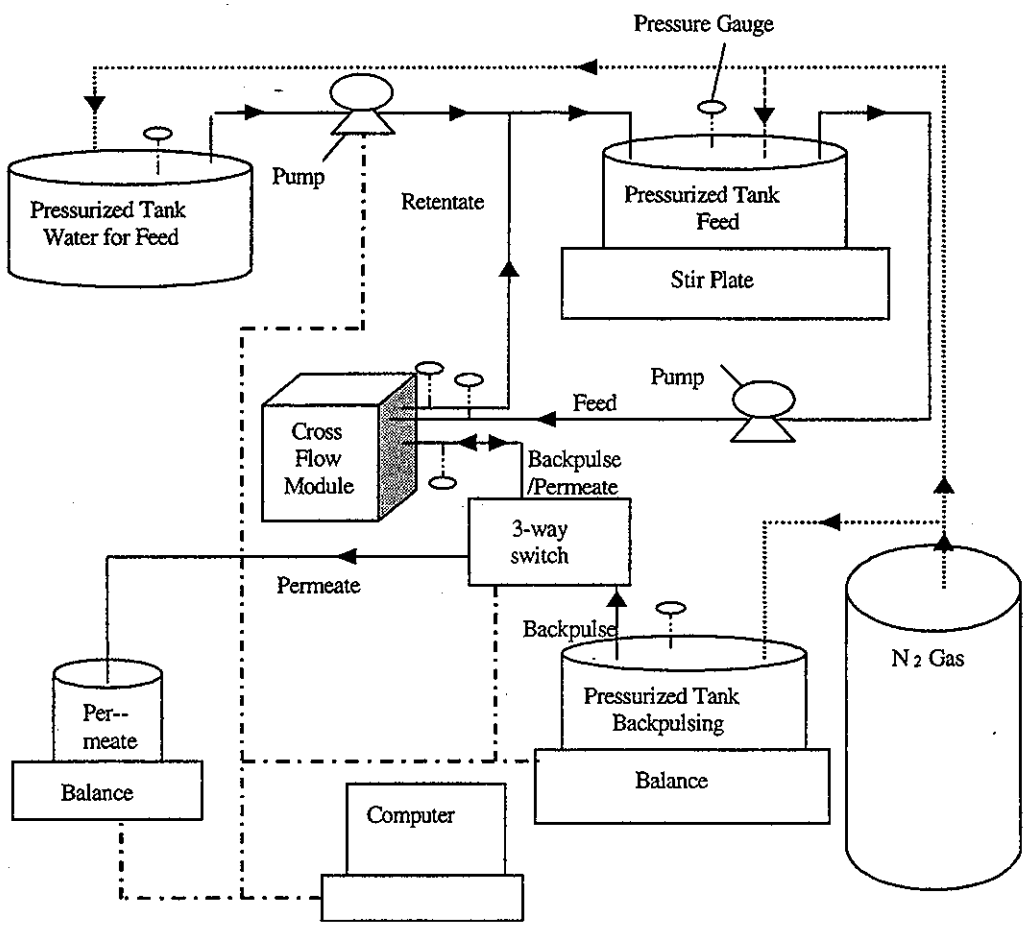

Figure 2. Schematic diagram of the crossflow filtration system. The solid lines depict liquid flows, the dotted lines depict gas flows, and the dashed-dotted lines depict electronic connections from the computer to a pump, the solenoid valve, and two balances (from Mores et al. (1999)).

3. RESULTS AND DISCUSSION

3.1 Photografting on Membrane Surfaces

It is well recognized that simultaneous photoinduced graft polymerization onto substrates occurs *via* hydrogen abstraction (Ulbricht et al., 1996; Yang and Ranby, 1996; Li et al., 1997). This principle suggests that excited benzophenone can abstract hydrogen in the absence of monomer to form the surface initiator, as proposed in Figure 1. A series of experiments has been conducted to provide evidence of the surface initiator formation in the first step of the process. The results are listed in Table 1. It is shown that the weight of the membranes did not change significantly without BP or without UV. However, the weight of the membranes did increase with BP coating and UV irradiation, and higher weight gain was obtained in nitrogen than in air. These results indicate that the reaction proceeded as desired and that the benzophenone (BP) was chemically bound to the substrate upon UV irradiation. Otherwise, the BP would be washed off from the substrate in a good solvent. There are two possible reasons for the weight gain. One reason is the formation of peroxide (Ulbricht et al., 1996; Uchida et al., 1993; Uyama and Ikada,

1988). the other is the formation of graft BP through hydrogen abstraction. The formation of peroxide is excluded in our experiments, since oxygen is an inhibitor. Additional evidence about surface initiator formation is provided in subsequent sections of this report.

Table 1. Weight percent gain of PP membranes and standard deviation for six repeats in air or nitrogen. 'Without BP' means that blank membranes without BP were irradiated 26.6 seconds (20 passes × 1.33 s.). 'Without UV' indicates that membranes were soaked in 5 wt% BP in benzene solution, without irradiation, and then soaked and washed in acetone and dried until constant weight. 'With BP and UV' means that the membranes were modified under the following conditions: 5 wt% BP in benzene, 26.6 seconds UV irradiation.

	Without BP	Without UV	With BP and UV
In Air	0.01 ± 0.02	0.02 ± 0.03	0.17 ± 0.03
In N_2	0.03 ± 0.03	0.02 ± 0.02	0.34 ± 0.02

Verification of initiative ability of surface initiator and living graft polymerization

From Table 2, significant weight gain in the second step of the process was obtained on the membrane with surface initiator and UV irradiation in nitrogen. The weight change is relatively small or not significantly different from zero at all other conditions. These results indicate that the oligomer or polymer was indeed grafted on the membranes. Homopolymerization of AA can occur with or without surface initiator in the presence of UV irradiation. However, the homopolymer formed in the absence of surface initiator is washed off in a good solvent. Thus, the weight gain of the membrane is caused by graft polymerization that was initiated by the surface radicals. The membrane weight was nearly unchanged when the UV irradiation was performed in the presence of air. This result suggests that oxygen is a strong inhibitor of the second step of the graft polymerization process, as expected, since oxygen is an inhibitor of free radical polymerizations.

As mentioned earlier, the semipinacol radicals prefer to combine with growing polymeric chain radicals. So, the termination pattern produces a grafted copolymer that is rooted on the surface of the polymer substrates and carries end groups which were also found to be able to reinitiate polymerization as reported by Yang and Ranby (1996). In fact, numerous experiments in our work also demonstrate that the growing chain radicals terminate the semipinacol radicals and then split-off to initiate polymerization to increase the graft polymer chain length.

Table 2. Weight percent gain of PP membranes and standard deviation for six repeats. The monomer solution for all membranes was 25 wt% AA in ethanol. UV irradiation time was 9.31 seconds (7 passes × 1.33 s). The grafted BP in the first step was 0.34 wt% of the blank PP membrane under the conditions of 5 wt% in BP in benzene and 26.6 s UV irradiation.

	Blank Membranes		Membranes with Surface Initiator	
	Without UV	With UV	Without UV	With UV
In Air	0.00 ± 0.00	0.02 ± 0.07	0.01 ± 0.01	0.01 ± 0.00
In N_2	0.01 ± 0.02	0.06 ± 0.04	0.02 ± 0.04	2.78 ± 0.32

Control of grafting density and average graft polymer chain length

Figure 3 shows the relationship between grafting density (mole of surface initiators per volume) and UV irradiation time at different BP solution concentrations. As expected, grafting density increases with increasing UV irradiation time and has a maximum value with increasing

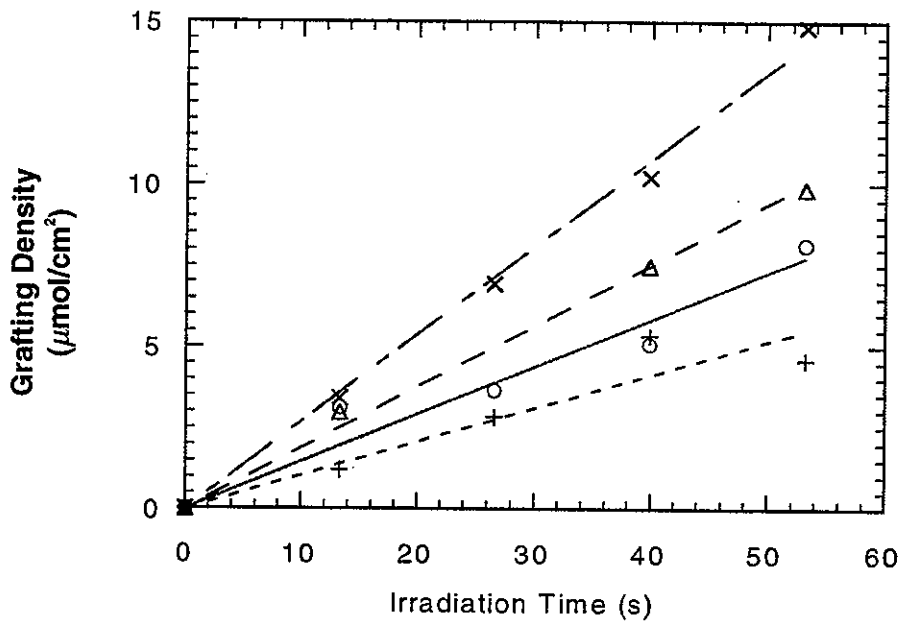

Figure 3. Grafting density versus irradiation time at different BP concentrations (o) 0.5 wt% BP; (×) 10 wt% BP; (Δ) 30 wt% BP; (+) 70 wt% BP.

BP concentration for a given UV irradiation time. Very low BP concentrations are undesired due to low surface initiation, whereas very high BP concentrations are undesired because BP absorbs the UV radiation. The results of Figure 3 indicate that the grafting density of the surface initiator can be controlled by controlling UV irradiation time and BP concentration.

In the second step of the novel photografting process, it is reasonable to assume that each surface initiator formed in the first step initiates polymerization to form one graft polymer chain since the surface initiator concentration is very low (0.34 wt% of the substrate) and the photoinitiation is very rapid. So, the average graft polymer chain length is calculated by equation (4). The results in Figure 4 demonstrate that the graft polymer chain length increases linearly with increasing UV irradiation time for a given grafting density and a given AA concentration. The graft polymer chain length also increases with increasing AA concentration in the ethanol solution. These results indicate that the graft polymer chain length can be controlled by adjusting irradiation time and monomer concentration, which is expected to have potential advantages in the membrane surface modification for controlling membrane fouling.

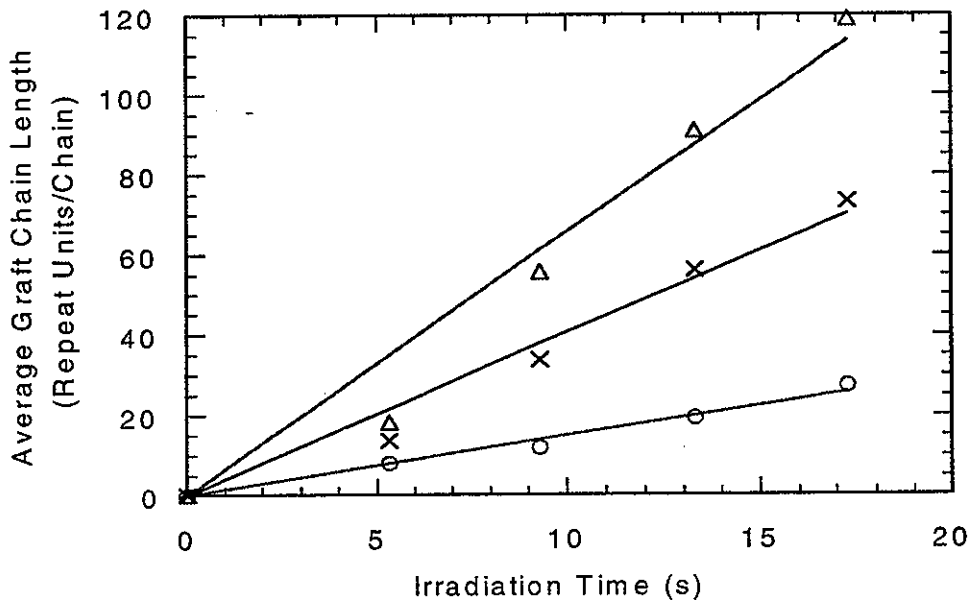

Figure 4. Average graft polymer chain length versus irradiation time at different AA concentrations; (o) 5 wt% AA; (×) 15 wt% AA; (Δ) 25 wt% AA. The amount of grafted BP in the first step was 0.34 wt% of the blank PP membrane under the conditions of wt% BP in benzene and 26.6 s UV irradiation for all experiments.

Comparison of sequential and simultaneous grafting methods

The simultaneous and novel sequential photoinduced grafting polymerization methods were both used to modify PP membranes and then compared. With 0.34 wt% BP grafted in the first step and 50 wt% AA in ethanol used in the second step, the grafting efficiency after 13.3 seconds of UV irradiation is 18 ± 3 % for the simultaneous method and 83 ± 6 % for the sequential method, at the 90% confidence level for three repeats. The conditions used for these experiments are ones which exaggerate the effects of lower efficiency in the simultaneous grafting case. Poly(acrylic acid) and monomeric acrylic acid both are very capable of hydrogen abstraction. When other monomers with less labile hydrogens are grafted or are grafted under different grafting conditions, the grafting efficiency may be much higher for the simultaneous grafting method (Yang and Ranby, 1996; Ranby et al., 1988).

For these studies, the grafting efficiency represents the percentage of grafted polymer relative to the total amount of polymer. It has been recognized that semipinacol radicals themselves rarely initiate bulk homopolymerization (Li et al., 1997). The significant percentage of homopolymer in the simultaneous method is attributed to the excited BP abstracting hydrogen from monomer to form monomer radicals, resulting in the formation of ungrafted homopolymer. Further, hydrogen abstraction from the graft polymer chain will result in the formation of branched or/and crosslinked polymer. In the novel sequential method, however, the homopolymer can be reduced significantly, and the formation of linear polymer chains is preferred, since there is no BP on the membrane surface or in the monomer solutions. The proposed reaction mechanism is confirmed by the fact that the grafting efficiency of the novel sequential method is 4-fold greater than that of the simultaneous method when AA was grafted to PP membranes in the present work. It is worth mentioning that the simultaneous grafting method is preferable when the hydrogen in the substrate is more readily abstracted by BP than is the

hydrogen in the monomer and in the newly formed grafted polymer or homopolymer. Under these conditions, the polymerization can be more efficient and simpler for the simultaneous method. Clearly, the photoefficiency in the simultaneous graft polymerization will be dramatically higher than the overall photoefficiency in the proposed process. Thus, the proposed process is particularly useful only for monomers (and graft copolymers) which readily abstract hydrogen, such as those studied in this work.

Reactions of a novel sequential photoinduced living graft polymerization

In this novel sequential photoinduced graft polymerization method, the grafting process can be divided into two steps: (1) synthesis of surface initiator, and (2) graft polymerization of monomers. In the first step, a BP molecule absorbs a photon and then abstracts a hydrogen atom from the substrate. This abstraction process creates surface radicals and semipinacol radicals. Because there is no monomer present in this step, the recombination of the surface radicals and semipinacol radicals takes place readily, and generates the surface initiators. The proposed reactions are described in equations (6)-(8):

$$(C_6H_5)_2C=O+h\gamma \xrightarrow{k_0'} (C_6H_5)_2C=O* \quad \text{photo excitation,} \tag{6}$$

$$(C_6H_5)_2C=O*+SH \rightarrow (C_6H_5)_2OHC\bullet+S\bullet \quad \text{hydrogen abstraction,} \tag{7}$$

$$(C_6H_5)_2OHC\bullet+S\bullet \rightarrow (C_6H_5)_2OHC-S \quad \text{surface initiator formation,} \tag{8}$$

where SH represents the substrate with hydrogen on the surface, * represents the excited state, and • stands for the radical.

In the second step, the substrate with the surface initiators grafted on its surfaces is exposed to the solution of monomer to be grafted and UV irradiation. The UV light cleaves the carbon-carbon bond of the surface initiator to form surface radicals and semipinacol radicals. The monomer reacts with surface radicals preferentially because of steric effects. Thus, the desired polymer chains can be grafted onto the substrate. The proposed reactions are listed in equations (9)-(12):

Photo excitation:

$$(C_6H_5)_2OHC-S+h\gamma \xrightarrow{k_0} (C_6H_5)_2OHC\bullet+S\bullet \quad \text{surface radical formation,} \tag{9}$$

Initiation:

$$S\bullet+M \xrightarrow{k_i} SM_1\bullet \quad \text{grafted monomer radical,} \tag{10}$$

Propagation:

$$SM_n\bullet+M \xrightarrow{k_p} SM_{n+1}\bullet \quad \text{grafted polymer radical,} \tag{11}$$

Termination:

$$SM_n\bullet+(C_6H_5)_2OHC\bullet \xrightarrow{k_t} SM_nC(C_6H_5)_2OH \quad \text{grafted polymer,} \tag{12}$$

where • stands for the radical and M represents monomer.

Kinetics of surface initiator formation

In terms of equations (6)-(8) and the Lambert-Beer law, the kinetic equation of surface initiator formation is written as

$$d_{[BPHS]}/dt = f\phi_S I_0 e^{-\varepsilon c[BP]}(1-e^{-\varepsilon b[BP]}), \tag{13}$$

where BPHS represents $(C_6H_5)_2OHC\text{-}S$ (the surface initiator formed in the hydrogen abstraction), f is surface initiator formation efficiency, ϕ_S is the quantum yield of surface initiator formation, I_0 is the intensity of incident UV irradiation, c is the thickness of a BP solution layer through which UV irradiation must pass to reach the substrate surface, and b is the thickness of the membrane where the hydrogen abstraction reaction occurs.

To determine the parameters in equation (13), experiments were performed using different BP concentrations at different irradiation times. The surface initiator formation rate can be obtained by taking the derivative of the amount of grafted BP with respect to irradiation time. It was found that the reaction rate is a constant for a given initial BP concentration. This behavior is predicted by equation (13) because the conversion of BP is very low and the BP concentration can be considered to be nearly constant.

The relationship between reaction rate and BP concentration is shown in Figure 5. There is an optimum BP concentration which maximizes the reaction rate, due to the reduction in UV transmittance to the membrane surface at high BP concentrations. The circles represent the experimental data while the solid line represents the best-fit of equation (13). The maximum likelihood estimate of the model parameters is obtained using KaleidaGraph™ based on the Levenberg-Marquardt (Press et al., 1992) method by minimizing the sum of the squared errors. The confidence intervals for the model parameters were calculated based on the work of Donaldson and Schnabel (1987), as suggested by Young et al. (1997). The best-fit model parameters and their 90% confidence intervals are $f\phi_S I_0 = 0.020 \pm 0.001$ mol/L·s, $\varepsilon c = 0.26 \pm 0.01$ ℓ/mol, and $\varepsilon b = 34 \pm 10$ L/mol.

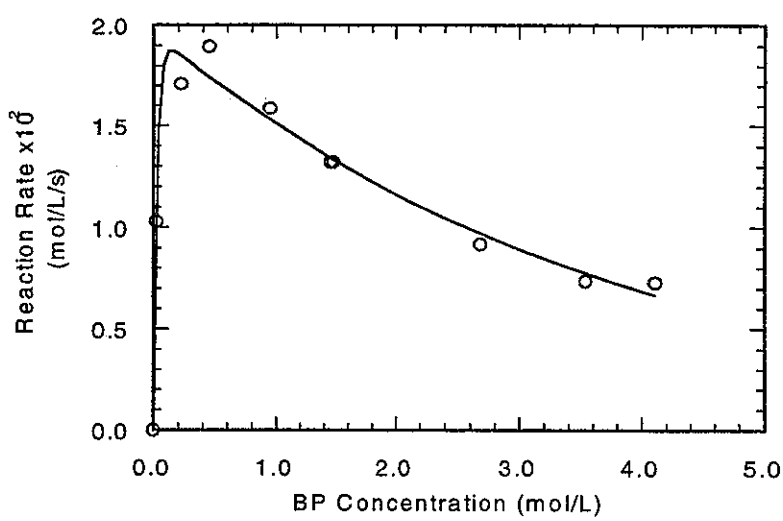

Figure 5. Reaction rates of initiator formation versus BP concentrations: (o) experimental data; (—) model curve. UV irradiation time is 26.6 s for all experiments.

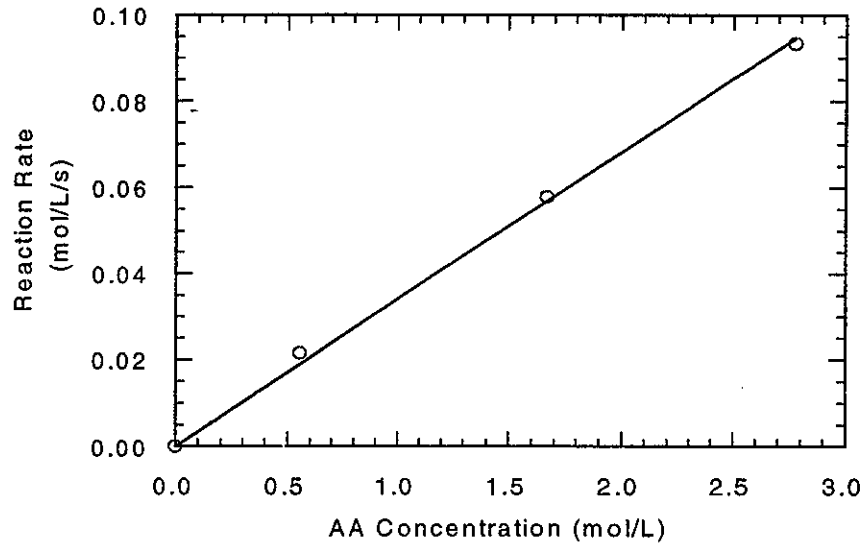

Figure 6. Reaction rates of graft polymerization versus AA concentration: (o) experimental data; (—) model curve. UV irradiation time is 26.6 s for all experiments. The amount of grafted BP in the first step was 0.34 wt% of the blank PP membrane under the conditions of 5 wt% BP in benzene and 26.6 s UV irradiation for all experiments.

Kinetics of living graft polymerization

According to equations (9)-(12), the kinetic equation for the second step can be written as

$$R_m = k_p[M]\{\phi I_0(1-e^{-\varepsilon b[BPHS]})/k_t\}^{1/2}, \quad (14)$$

where R_m represents the rate of monomer consumption, ϕ is the number of grafting chains produced per light photon absorbed, k_P and k_t are reaction rate constants, and [M] stands for the monomer solution concentration. To determine the quantitative relationship between reaction rate and monomer concentration, different monomer concentrations were used at different irradiation times. The monomer consumption rate was obtained by taking the derivative of the amount of grafted AA with respect to irradiation time. It was found that the reaction rate is a constant for each initial AA concentration. This behavior is predicted by equation (14), because the conversion of AA is very low, and the AA concentration can be considered to be nearly constant. The linear relationship between monomer consumption and reaction time further verifies the living graft polymerization.

The relationship between reaction rate and AA concentration is shown in Figure 6. The linear relationship of reaction rate and AA concentration confirms the proposed kinetic equation (14). The parameters in the graft polymerization rate equation were obtained using linear regression in KaleidaGraph™. Confidence intervals for the model parameters were calculated using the method reported by Walpole and Myers (1985). The best-fit slope and intercept as well as their 90% confidence intervals are 0.033 ± 0.002 s^{-1} and 0.001 ± 0.003 mol/L·s, respectively. As expected, the intercept is not significantly different from zero.

The parameters in equation (14) were obtained using the following method. The value of εb is 34 L/mol from the surface initiator formation kinetics, and [BPHS] is 0.014 mol/L in the

kinetic study of graft polymerization. The value of $k_p\{\phi I_0(1-e^{-\varepsilon b[BPHS]})/ k_t\}^{1/2}$ is 0.033 s^{-1} from the slope of the best-fit line in Figure 5. Therefore, $k_p\{\phi I_0/ k_t\}^{1/2}$ is 0.054 s^{-1} and the final kinetic equation for graft polymerization is $R_m= 0.054(1-e^{-34[BPHS]})^{1/2}[M]$, with [BPHS] and [M] having units of mol/L and R_m having units of mol/L·s.

Grafting on various polymer membranes

The two-step photoinduced grafting method was originally developed using PP microfiltration membrane as substrate and acrylic acid as monomer. To examine the effect of substrates on the graft polymerization, commercial cellulose acetate and polyvinylidene fluoride polymeric membranes were used in the experiments.

For the cellulose acetate (CA) microfiltration membrane, the results showing the effect of BP concentration on the surface initiator formation (1st step) are shown in Figure 7. As for the PP membrane, there is a maximum weight gain at an optimal BP concentration due to a competition between increased reaction rate and increased light attenuation with increasing BP concentration.

In the AA graft polymerization step (2nd step), the membranes with surface initiator weight gain from the first step of 0.27 ± 0.04 wt% were used at different AA concentrations. It was found that the membranes stuck to the glass plate and quartz disks when the AA concentration was 25 wt% or greater and the irradiation exposure was 10 passes or greater. The weight gains of the CA membrane were (5.8 ± 0.1) and (15.0 ± 0.2) wt%, respectively, for 5 wt% and 15 wt% AA in ethanol solutions at 10 passes. These results, shown in Figure 8, are likely caused by the large weight gains achieved when grafting to CA.

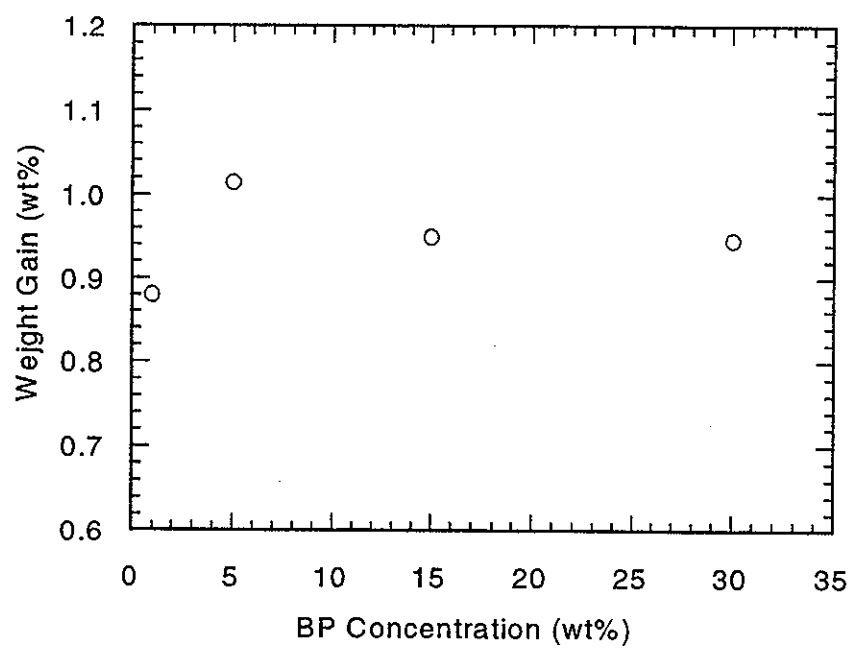

Figure 7. Amount of surface initiator vs. BP concentration. Average weight of CA membrane, 0.08 g. Irradiation time 10.6 seconds (8 passes).

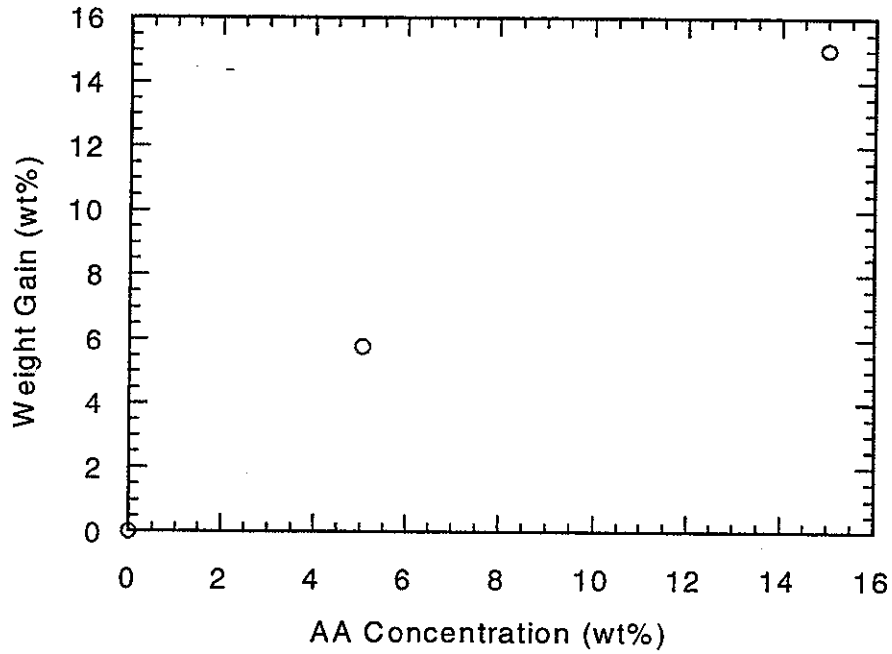

Figure 8. Weight gain as a function of AA concentration for graft polymerization on CA membranes. The amount of surface initiator formed in the first step was 0.27 ± 0.04 wr% and the UV irradiation time was 13 seconds.

For the polyvinylidene fluoride (PVDF) membranes, BP concentrations of 1–30 wt% in benzene and irradiation time of 20 passes were used in the surface initiator formation step. However, the weight change of modified PVDF was not large, and the second step was not performed.

For comparison, the results for all three membranes are presented in Table 3.

Table 3. Properties of Polymeric Membranes in Two-step Graft Polymerization

Substrates	Chemical Structure	Surface Initiator formation		Monomer Graft Polymerization	
		Irradiation Time (s)	Wt% Gain*	Irradiation Time (s)	Wt% Gain*
CA	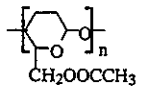 *	11	1.01 ± 0.14	13	15.0 ± 0.2
PP	$-(CH_2CH)_n-$ $\vert$ CH_3	13	0.16 ± 0.02	13	7.3 ± 0.5
PVDF	$-(CH_2CF_2)_n-$	106	0.08 ± 0.05	n/a	n/a

* Weight percent gain plus and minus one standard deviation for three repeats. BP solution was 5 wt% BP in benzene in the first step for all the membranes. In the second step, the monomer solution was 15 wt% AA in ethanol for all the membranes, and the amounts of grafted BP were 0.30 wt% and 0.27 wt% for PP and CA, respectively.

In the surface initiator formation (1st step), cellulose acetate (CA) has the highest reactivity due to the activating effect of the adjacent O atoms. Polypropylene contains a large number of tertiary hydrogen atoms which are easily abstracted by BP, and it has, therefore, a higher reactivity than that of poly(vinylidene fluoride) (PVDF) but a lower reactivity than that of CA. In the graft polymerization (2nd step), the carbon-carbon bond of the surface initiator in CA is more easily cleaved to form surface radicals and semipinacol radicals due to the activating effect of adjacent O atoms and so CA shows higher reactivity than does PP.

3.2 Membrane Performance

Figure 9 shows the pure buffer flux, plus and minus one standard deviation, for unmodified PP membranes, commercial CA membranes, and modified PP membranes with different amounts of grafted PEG200MA. The higher buffer flux for CA membranes (3100 ± 200 L/m^2 h) than that for the unmodified PP membranes (1100 ± 100 L/m^2 h) reflects the difference in membrane morphologies. The buffer flux is nearly the same for unmodified and modified PP membranes, which suggests that the bulk structure of PP membranes was not greatly altered by the surface modification process in the weight gain range (2-10 wt%) used in the experiments. However, there is a small but statistically significant (at the 95% confidence level) increase in the buffer flux at small weight gains (2-5%), suggesting that making the membrane surface hydrophilic improves wetting and helps eliminate microbubbles which inhibit flow. The buffer flux declines slightly at larger weight gains, most likely due to partial blockage of the membrane pores by the grafted polymer. The average buffer flux for the PP membranes modified with AA (7 repeats; weight gain 4 ± 0.2 wt%) and DMAEMA (8 repeats; weight gain 4 ± 1 wt%) are, respectively, 1130 ± 100 L/m^2 h and 1200 ± 120 L/m^2 h. These values are similar to those for unmodified PP and modified PP with PEG200MA.

Membranes were then tested in the crossflow filtration system without backpulsing using 0.14 g/L *E. coli* bacterial suspensions. As shown in Figure 10, the flux decreased quickly for all the membranes due to fouling. Although the flux for the CA membrane is initially more than twice that for the unmodified and modified PP membranes, it drops the most rapidly and becomes comparable to that of the other membranes within 1-2 minutes. For all membranes, the long-term flux after 60 min without backpulsing is only approximately 70 L/m^2 h. It is expected that the fouling is primarily due to physical deposition of the bacterial cells on the membrane surfaces, which is not strongly dependent on the membrane surface chemistry. For the unmodified PP membrane, the recovered flux after backwashing is seven times greater than long-term flux after one hour of filtration. For the modified PP membrane and the commercial CA membrane, the recovered fluxes are 10 times greater than long-term flux. These results indicate the potential for the membranes to be cleaned *in situ* using backpulsing.

Backpulsing experiments were then conducted at different backward and forward filtration durations, using unmodified PP membranes and 0.14 g/L bacteria. The results in Figure 11 for a fixed forward filtration duration of 4 sec show that the average net flux is maximized at a backpulse duration of approximately 0.15-0.20 sec. Longer backpulse durations are undesired due to unnecessary permeate loss, whereas shorter backpulse durations are undesired because the backpulse may be too short to effectively remove the foulants (Mores et al., 1999). The maximum average net flux with backpulsing in Figure 11 is about two-fold greater than that without backpulsing.

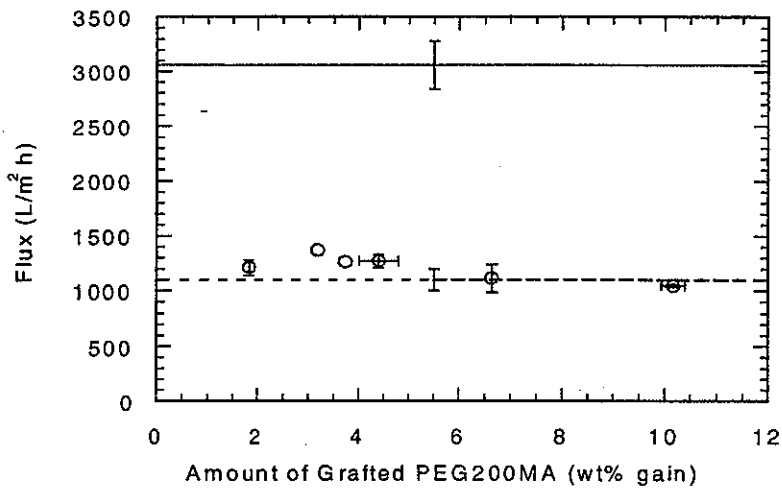

Figure 9. **Pure buffer flux at 5 psi versus the amount of grafted PEG200MA. The symbols are the pure buffer flux for PP membranes modified with PEG200MA (3-6 repeats). The dashed and solid lines show the pure buffer flux for the unmodified PP membrane (26 repeats) and CA membrane (7 repeats), respectively. The error bars represent plus and minus one standard deviation.**

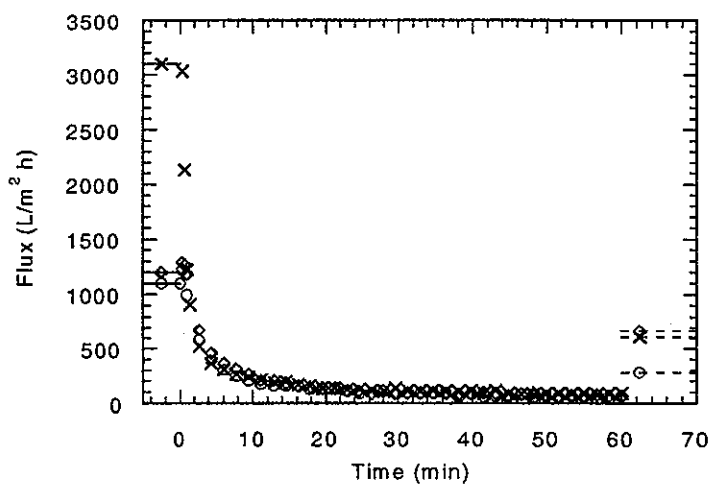

Figure 10. **Permeate flux versus filtration time of 0.14 g/L *E. coli* without backpulsing at a forward transmembrane pressure of 5 psi: (o) unmodified PP membranes (◊) PP membranes modified with 5 wt% weight gain of PEG200MA, and (×) commercial CA membranes. Also shown are the pure buffer fluxes for 5 minutes before filtration (solid lines) and 5 minutes after filtration and backwashing (dashed lines).**

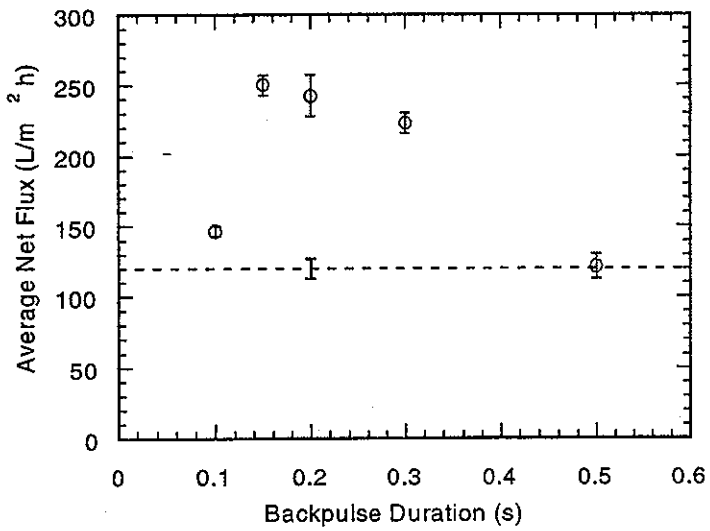

Figure 11. **Average neg flux (symbols) versus backpulse duration for crossflow filtration of 0.14 g/L *E. coli* at a forward filtration time of 4 seconds between backpulses, with forward transmembrane pressure of 5 psi and backward transmembrane pressure of 3 psi. The dashed line is the corresponding result without backpulsing. The error bars represent plus and minus one standard deviation for two or three repeats.**

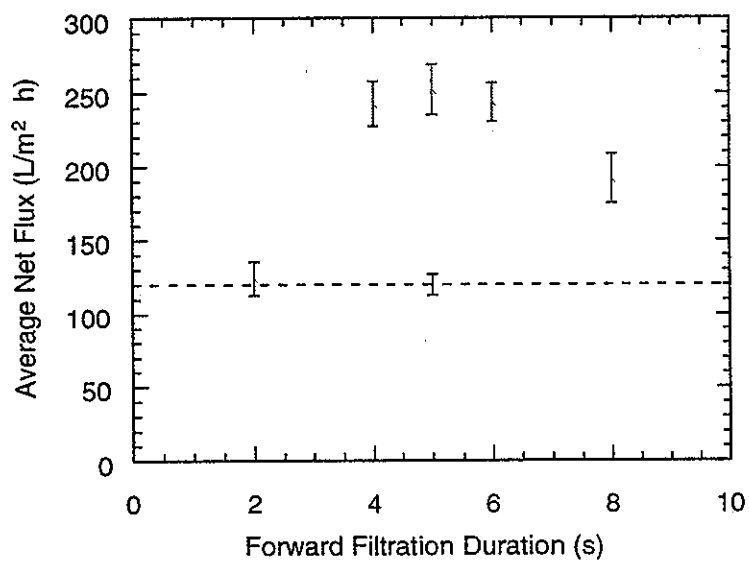

Figure 12. **Average net flux (symbols) versus forward filtration duration for crossflow filtration of 0.14 g/L *E. coli* at a fixed backpulse duration of 0.2 seconds, with forward transmembrane pressure of 5 psi and backward transmembrane pressure of 3 psi. The dashed line is the corresponding result without backpulsing. The error bars represent plus and minus one standard deviation for two or three repeats.**

The effects of varying forward filtration duration on the average net flux are shown in Figure 12 for a fixed backpulse duration of 0.2 sec. There is an optimum backpulsing frequency of once every 4-6 sec to maximize the average net flux. As reported by Redkar and Davis (1995), higher backpulse frequencies cause more permeate loss relative to that collected during the short periods of forward filtration. For lower backpulse frequencies, on the other hand, the average net flux decreases due to cake formation or fouling during the relatively long period of forward filtration.

The combination of surface modification and backpulsing was then tested to determine its effectiveness in reducing membrane fouling. Figure 13 shows the permeate volume versus filtration time with and without backpulsing for an unmodified PP membrane, PP membranes modified with different monomers, and an unmodified CA membrane. As discussed previously, the performance without backpulsing is nearly independent of the membrane surface chemistry and morphology, as it is primarily controlled by the bacterial cake which is deposited on the membrane surface. A very different result is observed with backpulsing, however. For the unmodified PP membrane (which is hydrophobic and neutral), the total permeate volume after 60 min of filtration with backpulsing is 1.7 times that obtained without backpulsing. In contrast, the total mass of the permeate after 60 min of filtration with backpulsing using the PP membrane modified with PEG200MA (which is hydrophilic and neutral) is 2.6 times that obtained without modification and backpulsing. The higher flux enhancement obtained for the modified PP membrane demonstrates that the membrane fouling is reduced further by an effective combination of backpulsing and surface modification. These results suggest that the adhesive

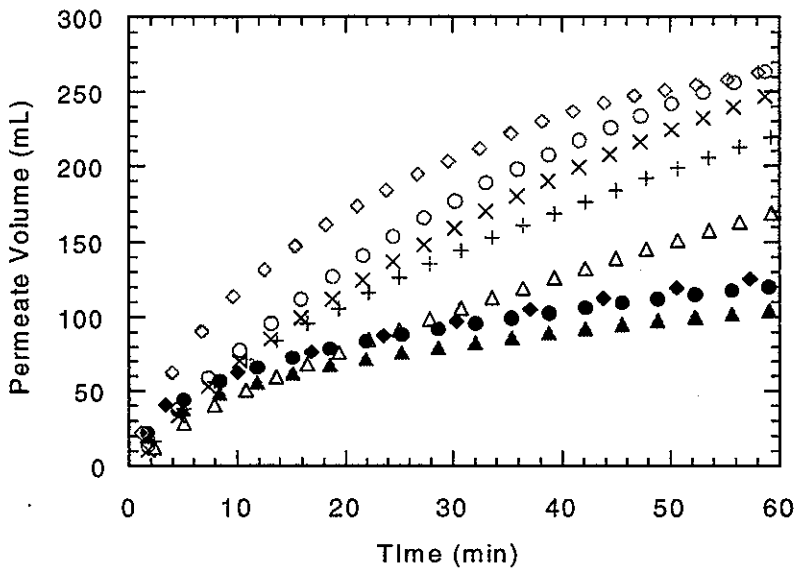

Figure 13. Permeate volume verses filtration time for crossflow filtration of 0.14 g/L *E. coli*: (o), (×), (+) backpulsing results for PP membranes modified with weight gain of 4.4 wt% PEG200MA graft, 4.4 wt% AA graft, and 3.7 wt% DMAEMA graft, respectively; (Δ), (▲) unmodified PP membranes with and without backpulsing, respectively; (•) PP membrane modified with weight gain of 5.8 wt% PEG200MA and without backpulsing; (◊), (♦) unmodified CA membranes with and without backpulsing, respectively. Backpulsing experiments were performed at backward transmembrane pressure of 3.0 psi for 0.2 seconds after every 4 seconds of forward filtration at a transmembrane pressure of 5.0 psi.

hydrophobic interactions are stronger than the hydrophilic ones (Marshall, 1985) between the bacteria and the membrane surfaces, so that the bacteria are more easily lifted off the modified membrane during each backpulse. The relatively high permeate collection for the CA membrane (which is hydrophilic and neutral) with backpulsing supports this observation.

Figure 13 also shows that the permeate collection for the PP membranes modified with AA (hydrophilic, negatively charged) and DMAEMA (hydrophilic, positively charged) is greater than that for the unmodified PP membrane (hydrophobic, neutral), but less than that for the PP membrane modified with PEG200MA (hydrophilic, neutral) and the unmodified CA membrane (hydrophilic, neutral). Since *E. coli* has both negatively and positively charged surface groups (Brock and Madigan, 1991), it is not surprising that the neutral hydrophilic membrane surfaces are the most effective in reducing *E. coli* fouling.

Table 4 shows the long-term flux without backpulsing, the long-term net flux with backpulsing, and the recovered flux after backwashing for unmodified PP membranes, PP membranes modified with different monomers, and commercial CA membranes. The long-term flux values without backpulsing are nearly the same for all the membranes, indicating that physical deposition of bacteria on the membrane is the dominant fouling mechanism and that the membrane surface chemistry is then of less importance. On the other hand, the recovered fluxes for the modified PP membranes and the CA membrane are higher than that for the unmodified PP membrane, providing further evidence that the adhesive interactions of the bacteria with the hydrophilic membrane surfaces are weaker than those with a hydrophobic surface.

Table 4. Effect of membrane surface chemistry on long-term flux and recovered flux after backwashing, with and without backpulsing. Shown are the average plus and minus one standard deviation for 2-6 repeats.

Membrane	Without Backpulsing		With Backpulsing	
	Long-term Flux (L/m^2h)	Recovered Flux (L/m^2h)	Long-term Net Flux (L/m^2h)	Recovered Flux (L/m^2h)
Unmodified PP	64 ± 5	280 ± 50	130 ± 20	210 ± 10
Unmodified CA	77 ± 5	610 ± 70	160 ± 10	400 ± 40
PP + 5.0 wt% PEG200MA	67 ± 4	670 ± 40	150 ± 20	380 ± 20
PP + 4.4 wt% AA	64 ± 5	610 ± 50	140 ± 10	320 ± 10
PP + 3.7 wt% DMAEMA	66 ± 5	620 ± 70	130 ± 10	310 ± 30

The long-term net flux values with backpulsing in all cases are about twice those without backpulsing. However, the increase in the long-term fluxes with surface modification is relatively small. Apparently, surface modification in combination with backpulsing is most effective for short filtration times (see Figure 13) when the membrane surfaces are relatively clean, but by one hour the membranes are sufficiently fouled that the resulting long-term flux is controlled more by the foulant deposition than by the clean membrane surface properties. Nevertheless, the foulant is most easily removed by backpulsing from the neutral hydrophilic surfaces, leading to higher recovered fluxes than for the hydrophobic unmodified PP membrane or for the modified membranes with negative (AA) and positive (DMAEMA) charges.

Another result shown in Table 4 is that the recovered fluxes for the PP membranes fouled without backpulsing are greater than those with backpulsing. The fouling without backpulsing is expected to be primarily in the form of a cake layer of rejected *E. coli* cells. The cake layer on the membrane surface may then play the role of a secondary membrane to capture smaller particles, such as extracellular proteins and broken cells, and prevent them from blocking the membrane pores (Kuberkar et al., 1998). For filtration with backpulsing, however, the

backpulsing lifts a portion of the deposit off the membrane with high frequency. After each backpulse, with the cake removed from parts of the membrane surface, the small particles may then enter the membrane pores and cause internal fouling which may not be subsequently removed by backwashing.

The effects of the amount of grafted PEG200MA on the permeate fluxes were also examined. As shown in Figure 14, the long-term flux and the recovered flux for modified PP membranes do not change significantly with the amount of grafted PEG200MA in the weight gain range of 1.8 –10 wt%. Apparently, the increased hydrophilicity of the membrane with increased graft is offset by slight pore constriction from the grafted polymer.

Finally, different concentrations of *E. coli* were used in the backpulsing experiments for both unmodified and modified PP membranes, and the results are summarized in Table 5. The average net flux, long-term net flux with backpulsing, and the recovered flux after backwashing decreased with increasing *E. coli* concentration, as expected (Parnham and Davis, 1995; Kuberkar et al., 1998). The enhancement of the net flux due to the surface modification is most significant at low concentrations of foulant. At higher concentrations, a thicker cake layer forms and so the membrane surface chemistry is less important. However, the recovered flux is always higher for the modified membranes, indicating that backpulsing is able to lift the deposit more easily off the hydrophilic membrane than off the hydrophobic membrane.

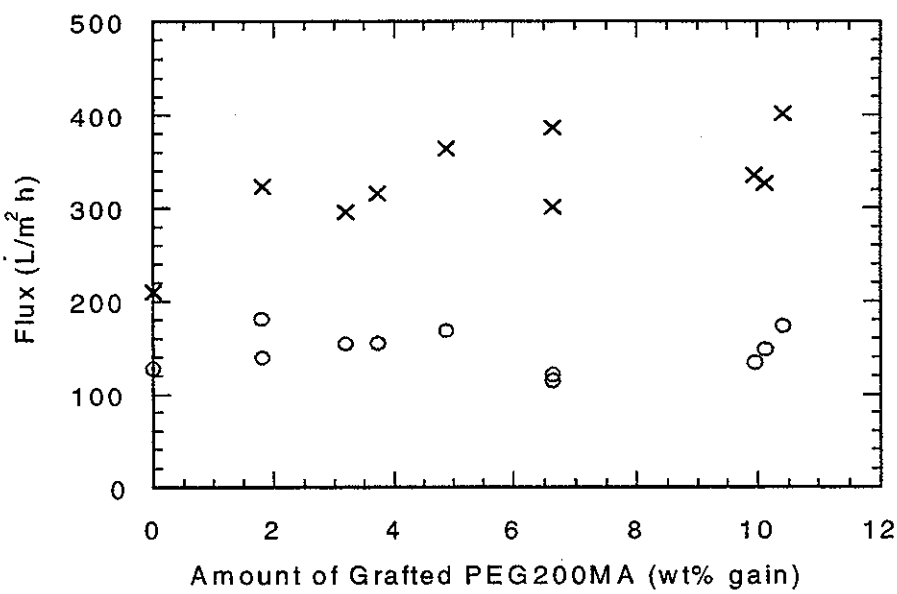

Figure 14. Long-term net flux with backpulsing (o) and recovered flux after backwashing (×) versus the amount of grafted PEG200MA for crossflow filtration of 0.14 g/L *E. coli*. These experiments were performed at a backward transmembrane pressure of 3.0 psi for 0.2 seconds after every 4 second of forward filtration at a transmembrane pressure of 5.0 psi.

Table 5. Effects of *E. coli* concentration on the average net flux with backpulsing, long-term net flux with backpulsing and recovered flux after backwashing for unmodified PP membranes and modified PP membranes with a weight gain of 3.5 wt% PEG200MA. Shown are the averages plus and minus one standard deviation for 2-4 repeats.

E. coli (g/L)	Average Net Flux (L/m^2h)		Long-term Net Flux (L/m^2h)		Recovered Flux (L/m^2h)	
	PP	PP + PEG	PP	PP + PEG	PP	PP + PEG
0.05	270 ± 20	440 ± 40	160 ± 10	280 ± 30	310 ± 30	480 ± 60
0.14	240 ± 15	330 ± 15	130 ± 20	150 ± 20	210 ± 10	380 ± 20
0.62	90 ± 10	120 ± 10	70 ± 10	70 ± 10	170 ± 10	310 ± 30

3.3 Fundamental Analysis of Membrane Fouling

To obtain a more fundamental understanding of backpulsing and membrane-foulant interactions, experiments were completed to examine how the reverse flow during each backpulse is able to remove the nonadhesive foulants from the membrane surface. In the first type of experiment, bacteria were deposited on commercial cellulose-acetate membranes, and then a single backpulse of a specified strength and duration was imposed. The flux recovery was then measured to determine how much of the foulant was removed. It was found that the fractional flux recovery increased with backpulse duration and strength and then saturated at a maximum value. The fraction β of the foulant cake removed versus time during a backpulse is well-described by a single exponential rise:

$$\beta(t) = \beta_{max}\left(1 - e^{-t/\tau_b}\right) , \tag{15}$$

where β_{max} is the nonadhesive foulant fraction and τ_b is the time constant for cake removal during reverse filtration. A model was then developed for the cyclic process of forward and reverse filtration and shown to provide good agreement with the net flux for rapid backpulsing experiments and to predict the optimal backpulse duration and frequency (Mores et al., 1999).

Figure 15 below shows a schematic of the partial membrane cleaning during a backpulse, and Figure 16 shows the model prediction and experimental verification of an optimum duration

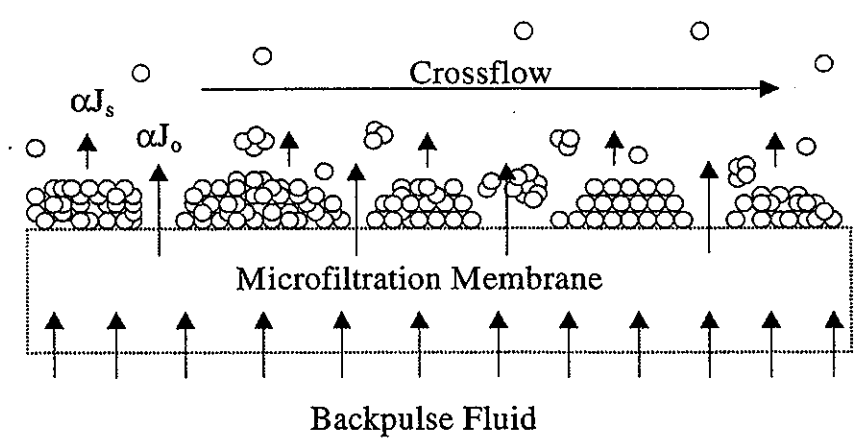

Figure 15: Schematic of partial cake removal by backpulsing; J_o is the clean membrane flux, J_s is the fouled membrane flux, and α is the ratio of transmembrane pressures during backpulse and forward filtration.

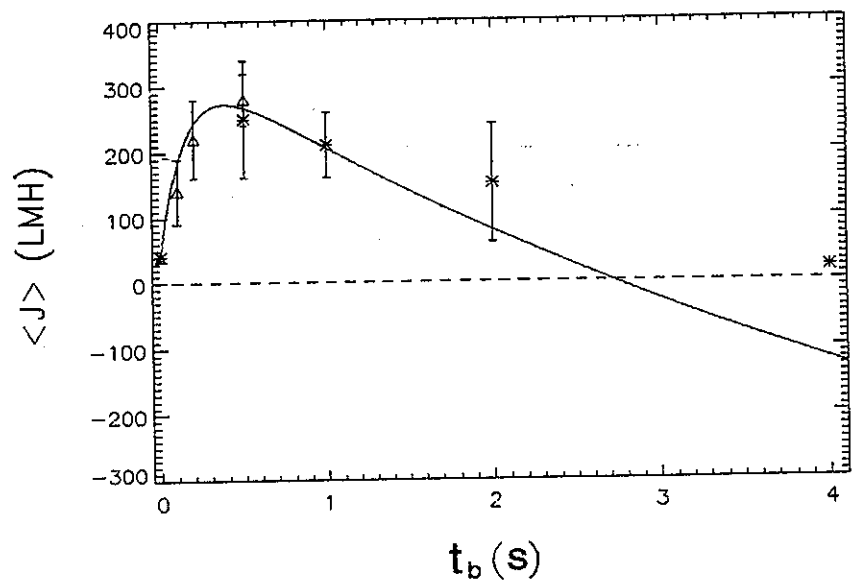

Figure 16: Experimental data and model prediction of the net flux versus the duration of each backpulse for crossflow microfiltration of 1.0 g/L *E. coli* bacteria using 0.2 μm cellulose-acetate membranes and a forward filtration period of 10 s between each backpulse.

whereas too much fluid is lost from the permeate side to the feed side if the backpulses are too long. Only 19% of the bacterial fouling was found to be reversible.

Experiments on commercial cellulose-acetate membranes were also completed with complex mixtures containing multiple foulants which led to simultaneous internal fouling (pore plugging) and external fouling (cake formation). Using yeast cells and protein as a model mixture, microfiltration was performed using both deadend and crossflow filtration devices (Güell et al., 1999; Kuberkar and Davis, 1999a). In both cases, the internal fouling by protein aggregates was reduced by the formation of the external fouling layer. A model of simultaneous internal and external fouling was developed, with the external cake layer of large particles serving as a dynamic secondary membrane or deep-bed filter that captures the smaller particles which would otherwise foul the pores of the primary membrane (Kuberkar and Davis, 1999b).

3.4 Economic Analysis and Comparisons

The economic analysis is adapted from the work of Ramirez and Davis (1998) for the removal of fine particles and microorganisms from wastewater. The total costs include both capital and operating costs.

The annualized capital costs per unit treated volume are calculated from an expression developed by (Wiesner et al., 1994):

$$cc = \left(C_{mod} N_{mod} + \$1.50 \times 10^5 N_{mod}^{0.74}\right)(AF / Q) \quad , \tag{16}$$

where $AF = 0.10$ year^{-1} is the amortization factor, Q is the volumetric treatment rate, N_{mod} is the number of modules required, and C_{mod} = \$14,600 is the cost of a single membrane module. The first term in the numerator is the membrane-related cost (housing and initial membranes), and the second term is the nonmembrane cost (pumps, valves, piping, etc.).

The primary operating costs include power (for pumping feed, recycling retentate, and backpulsing), membrane replacement, maintenance, and labor. These costs were determined from Pickering and Wiesner (1993) and Peters and Timmerhaus (1991).

Both capital and operating costs depend strongly on the number of membrane modules, which is directly related to the amount of membrane surface area required. The latter is given by

$$A = Q/\langle J \rangle \quad , \tag{17}$$

where $\langle J \rangle$ is the average net permeate flux. Figure 17 shows the total cost of membrane-treated water versus the net membrane flux for small (Q = 0.5 million gallons per day, MGD) and large (Q = 10 MGD) treatment facilities. When the net flux is less than approximately 200 L/m^2-h, the cost becomes noncompetitive with conventional treatment, for which the total cost is approximately \$0.8/m^3 for a 0.5 MGD facility (Owen et al., 1995). When the net flux is increased, the total costs decrease due to the reduced amount of membranes required. The total costs for systems employing backpulsing and membrane surface modification will be lower because of the higher net flux achieved. The additional capital costs to implement backpulsing are small, since normal installations have the necessary pumps and piping for reverse flow for cleaning purposes. Also, modified membranes are expected to have similar or lower price per area as compared to current commercial membranes, because inexpensive base membrane materials such as polypropylene may be used.

From Tables 4 and 5, the long-term flux for bacteria in our studies varies from about 70 L/m^2-h without backpulsing to as much as 280 L/m^2-h with surface modification and backpulsing. The greatest improvement occurs for dilute suspensions which are typical of wastewater. Table 6 shows the approximate flux values and associated cost for a 0.5 MGD membrane facility using 0.05 g/L *E. coli* as the foulant. Compared to the estimated cost of \$0.8/m^3 for conventional treatment, the modified membrane with backpulsing saves approximately \$0.25/m^3 (\$1/1000 gallons). Higher net fluxes may be obtained by optimizing the transmembrane pressure, since increasing transmembrane pressure increases the driving force for both filtration and fouling. The commercial cellulose acetate membrane performs almost the same as the modified polypropylene membrane, but the latter is expected to have lower raw materials costs.

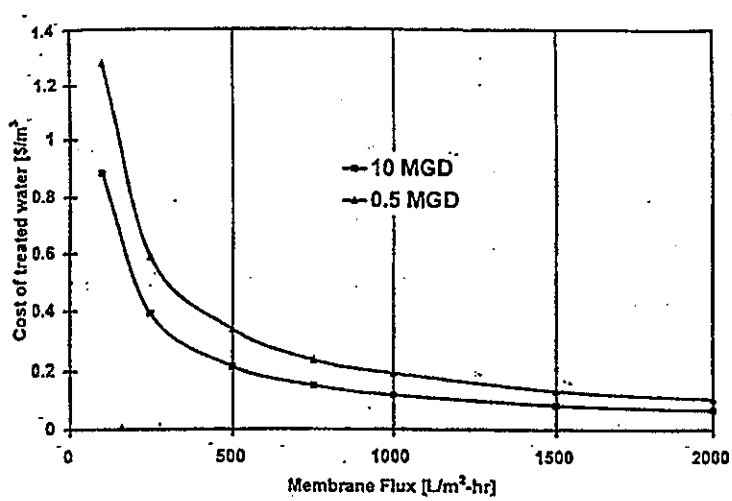

Figure 17. Total cost of treated water as a function of the average net permeate flux for 0.5 MGD and 10 MGD membrane treatment facilities.

Table 6. Long-term net flux and treatment cost for removal of 0.05 g/L bacteria from water by crossflow membrane microfiltration using unmodified and modified polypropylene membranes with and without backpulsing. PEG200MA with 3.5 wt% gain was used for the membrane surface modification.

	Flux (L/m^2-h)	Cost ($\$/m^3$)
Unmodified PP w/o Backpulsing	100	1.25
Unmodified PP w/Backpulsing	160	0.95
Modified PP w/Backpulsing	280	0.55

4 CONCLUSIONS

The combination of backpulsing and surface modification provides an effective method for reducing membrane fouling. A novel sequential photografting technique was developed for membrane surface modification. Desired membrane surface characteristics such as hydrophilicity and varied ionic charges were obtained by grafting different monomers to polypropylene base membranes using the novel grafting method. The experiments demonstrated that other membranes can also be modified using the novel grafting method with different monomers. For filtering 0.14 g/L *E. coli* using polypropylene membranes, 1.7-fold and 2.6-fold enhancements in the permeate volume collected over one hour were obtained using backpulsing alone and a combination of backpulsing and surface modification, respectively.

REFERENCE LIST

Al-Malack, M.H., and G.K. Anderson, Coagulation-crossflow Microfiltration of Domestic Wastewater, *J. Mem. Sci.* **121** (1996) 59-70.

Bowen, W.R., and H.A. Sabuni, Pulsed Electrochemical Cleaning of Cellulose Nitrate Microfiltration Membrane, *Ind. Eng. Chem. Res.* **31** (1992) 515-523.

Brock, T.D. and M.T. Madigan, *Biology of Microorganisms*, 6th Prentice Hall, Inc., New Jersey, 1991.

Cabassud, C., S. Laborie, and J.M. Laine, How Slug Flow Can Enhance the Ultrafiltration Flux in Organic Hollow Fibres, *J. Mem. Sci.* **128** (1997) 93-101.

Chung, K.Y., R. Bates, and G. Belfort, Dean Vortices with Wall Flux in a Curved Channel Membrane System, *J. Mem. Sci.* **81** (1993) 139-150.

Donaldson, J.R. and R.B. Schnabel, *Technometerics* **29** (1987) 67.

Güell, C., P. Czekaj, and R.H. Davis, Microfiltration of Protein Mixtures and the Effects of Yeast on Membrane Fouling, *J. Mem. Sci.* **155** (1999) 113-122.

Hvid, K.B., P.S. Nielsen, and F.F. Stengaard, Preparation and Characterization of a New Ultrafiltration Membrane, *J. Mem. Sci.* **53** (1990) 189-202.

Jonsson, A., and B. Jonsson, The Influence of Nonionic Surfactants on Hydrophobic and Ultrafiltration Membranes, *J. Mem. Sci.* **56** (1991) 49-76.

Keszler, B., G. Kovacs, A. Toth, I. Bertoti, and M. Hegyi, Modified Polyethersulfone Membranes, *J. Mem. Sci.* **62** (1991) 201-210.

Kim, K.J., A.G. Fane, and C.J.D. Fell, The Effect of Langmuir-Blodgett Layer Pretreatment on the Performance of Ultrafiltration Membranes, *J. Mem. Sci.* **43** (1989) 187-204.

Kim, K.J., A.G. Fane, and C.J.D. Fell, The Performance of Ultrafiltration Membranes Pretreated by Polymers, *Desalination* **70** (1988) 229-249.

Kim, M., K. Saito, and S. Furusaki, Water Flux and Protein Adsorption of a Hollow Fiber Modified with Hydroxyl Groups, *J. Mem. Sci.* **56** (1991) 289-302.

Kroner, K.H., H. Schutte, H. Hustedt, and M.R. Kula, Cross-flow Filtration in the Downstream Processing of Enzymes, *Proc. Biochem.* **19** (1984) (4) 67-74.

Kuberkar, V., P. Czekaj, and R.H. Davis, Flux Enhancement for Membrane Filtration of Bacterial Suspensions Using High-frequency Backpulsing, *Biotech. Bioeng.* **60** (1998) 77-87.

Kuberkar, V.T. and R.H. Davis, Modeling of Fouling Reduction by Secondary Membranes, *J. Mem. Sci.* (1999b, in press).

Kuberkar, V.T. and R.H. Davis, Effects of Added Yeast on Protein Transmission and Flux in Crossflow Membrane Microfiltration, *Biotech. Prog.* **15** (1999a) 472-479.

Kuruzovich, J.N., and P.R. Piergiovanni, Yeast Cell Microfiltration: Optimization of Backwashing for Delicate Membranes, *J. Mem. Sci.* **112** (1996) 241-247.

Li, Y., J.M. Desimone, C.D. Poon, and E. Samulski, *J. Appl. Polym. Sci.* **64** (1997) 883.

Ma, H., R.H. Davis, and C.N. Bowman, A Novel Sequential Photoinduced Living Graft Polymerization, *Macromolecules*, in press (1999).

Marshall, K.C., *Bacterial Adhesion: Mechanism and Physiological Significance: Mechanisms of Bacterial Adhesion at Solid-Water Interfaces*, Editors: D.C. Savage and M. Fletcher, Plenum Press, New York, 1985.

Matsumoto, K., S. Katsuyama, and H. Ohya, Cross-flow Filtration of Yeast by Microporous Ceramic Membrane with Backpulsing, *J. Ferment. Technol.* **66** (1988) 199-205.

Matsumoto, K., S. Katsuyama, and H. Ohya, Separation of Yeast by Cross-flow Filtration with Backpulsing, *J. Ferment. Technol.* **65** (1987) 77-83.

Mores, W.D., C.N. Bowman, and R.H. Davis, Theoretical and Experimental Flux Maximization by Optimization of Backpulsing, *J. Mem. Sci.* in press (1999).

Nakanishi, K., and H.G. Kessler, Stability and Rinsing Behavior of Deposited Layers, *J. Food Sci.* **50** (1985) 1726.

Nikolov, N.D., V. Mavrov, and J.D. Nikolova, Ultrafiltration in a Tubular Membrane under Simultaneous Action of Pulsating Pressures in Permeate and Feed Solution, *J. Mem. Sci.* **83** (1993) 167-172.

Nipkow, A., J.G. Zeikus, and P. Gerhardt, Microfiltration Cell-recycle Pilot System for Continuous Thermoanaerobic Production of Exo-•-amylase, *Biotech. Bioeng.* **34** (1989) 1075-1084.

Nystrom, M., and P. Jarvinen, Modification of Polysulfone Ultrafiltration Membranes with UV Irradiation and Hydrophilicity Increasing Agents, *J. Mem. Sci.* **60** (1991) 275-296.

Owen, G., M. Bandi, J.A. Howell, and S.J. Churchouse, Economic Assessment of Membrane Processes for Water and Wastewater Treatment, *J. Mem. Sci.* **102** (1995) 77.

Parnham, C.S., and R.H. Davis, Protein Recovery from Bacterial Cell Debris Using Crossflow Microfiltration with Backpulsing, *J. Mem. Sci.* **118** (1996) 259-268.

Parnham, C.S., and R.H. Davis, Protein Recovery from Cell Debris Using Rotary and Tangential Crossflow Microfiltration, *Biotech. Bioeng.* **47** (1995) 155-164.

Parvatiyar, M.G., Interaction of Dispersed Phase with Concentration Polarization, *J. Mem. Sci.* **115** (1996) 121-127.

Peters, M.S. and K.D. Timmerhaus, *Plant Design and Economics for Chemical Engineers*, 4th ed., McGraw-Hill, New York, 1991, p. 198.

Pickering, K.D. and M.R. Wiesner, Cost Model for Low-pressure Membrane Filtration, *J. Environ. Eng.* **199** (1993) 772.

Press, W.H., S.A. Teukdsky, W.T. Vetterling, and B.P. Plannery, in *Numerical Recipes in C*, 2nd ed., Cambridge University Press: Cambridge, 1992.

Ramirez, J.A. and R.H. Davis, Application of Cross-Flow Microfiltration with Rapid Backpulsing to Wastewater Treatment, *J. Haz. Mat.* **63** (1998) 179-197.

Ranby, B., Z.M. Gao, and P.Y. Zhang, *Polym. Prep. Am. Chem. Soc.* **27** (1988) 38.

Redkar, S.G., and R.H. Davis, Cross-flow Microfiltration with High-frequency Reverse Filtration, *AIChE J.* **41** (1995) 501-508.

Rodgers, V.G.J., and R.E. Sparks, Effects of Solution Properties on Polarization Redevelopment and Flux in Pressure Pulsed Ultrafiltration, *J. Mem. Sci.* **78** (1993) 163-180.

Rodgers, V.G.J., and R.E. Sparks, Effects of Transmembrane Pressure Pulsing on Concentration Polarization, *J. Mem. Sci.* **68** (1992) 149-168.

Rodgers, V.G.J., and R.E. Sparks, Reduction of Membrane Fouling in the Ultrafiltration of Binary Protein Mixtures, *AIChE J.* **37** (1991) 1517-1528.

Sambrook, J., E.F. Fritsch, and T. Maniatis, *Molecular Cloning-A Laboratory Manual*, Second Edition Cold Spring Hārbor Laboratory Press, 1989.

Si-Hassen, D., A. Ould-Dris, M.Y. Jaffrin, and Y.K. Benkahla, Optimisation of an Intermittent Cross-flow Filtration Process of Mineral Suspensions, *J. Mem. Sci.* **118** (1996) 185-198.

Stengaard, F.F., Characteristics and Performance of New Types of Ultrafiltration Membranes with Chemically Modified Surfaces, *Desalination* **70** (1988) 207-224.

Su, S.K., J.C. Liu, and R.C. Wiley, Cross-flow Microfiltration with Gas Backwash of Apple Juice, *J. Food Sci.* **58** (1993) 639-641.

Uchida, E., Y. Uyama, and Y. Ikada, *J. Appl. Polym. Sci.* **47** (1993) 417.

Ulbricht, M., H. Matuschewski, A. Oechel, and H.G. Hicke, Photo-Induced Graft Polymerization Surface Modification for the Preparation of Hydrophilic and Low-protein-adsorbing Ultrafiltration Membranes, *J. Mem. Sci.* **115** (1996) 31-47.

Uyama, Y. and Y. Ikada, *J. Appl. Polym. Sci.* **36** (1988), 1087.

Walpole, R.E. and R.H. Myers, In *Probability and Statistics for Engineers and Scientists*, 3rd ed., Macmillan Publishing Co., Inc.: New York, 1985.

Wenten, I.G., Mechanism and Control of Fouling in Crossflow Microfiltration, *Filt. Sep.* March issue (1995) 252-253.

Wiesner, M.R., J. Hackey, S. Sandeep, J.G. Jacangelo, and J.M. Laine, Cost Estimates for Membrane Filtration and Conventional Treatment, *J. Am. Water Work Assoc.* **86** (1994) (12) 33-41.

Wiesner, M.R., J. Hackney, S. Sethi, J.G. Jacangelo, and J.M. Laine, Cost Estimates for Membrane Filtration and Conventional Treatment, *J. AWAA* **85** (1994) 33.

Yamagishi, H., J.V. Crivello, and G. Belfort, Development of a Novel Photochemical Technique for Modifying Poly(arysulfone) Ultrafiltration Membranes, *J. Mem. Sci.* **105** (1995) 237-247.

Yamagishi, H., J.V. Crivello, and G. Belfort, Evaluation of Ultrafiltration Membranes, *J. Mem. Sci.* **105** (1995) 249-259.

Yan, W., P. Yang, and Y. Wang, UV-Radiation Grafting of Acrylamide onto Cellulose Acetate Reverse Osmosis Membrane, *Shuichuli Jishu* (in Chinese) **14** (1988) 213-222.

Yang, W. and B. Ranby, *J. Appl. Polym. Sci.* **62** (1996) 533.

Yang, W. and B. Ranby, *Macromolecules* **29** (1996) 3308.

Young, J.S., W.F. Ramirez, and R.H. Davis, *Biotech. Bioeng.* **56** (1997) 214.

Zahka, J., and T.J. Leary, Practical Aspects of Tangential Flow Filtration in Cell Separations, Purification of Fermentation Products, *ACS Symposium Series* **271** (1985) 51-69.

Zeman, L.J., and A. Zydney, *Microfiltration and Ultrafiltration: Principles and Applications*, Marcel Dekker, Inc., New York, 1996.

APPENDIX: DATA RECORD

Data for Figure 3

Time	0.5 wt%	10 wt%	30 wt%	70 wt%
0	0	0	0	0
13.3	3.1229	3.4179	2.9732	1.1966
26.6	3.6549	6.9269		2.847
39.9	5.07	10.212	7.4958	5.3451
53.2	8.1562	14.852	9.8726	4.5873

Data for Figure 4

Time	5 wt%	15 wt%	25 wt%
0	0	0	0
5.32	7.9554	13.702	18.22
9.31	11.957	33.641	55.712
13.3	19.392	56.186	91.073
17.29	27.426	73.379	118.93

Data for Figure 5

BP Conc.	Rate
0	0
0.02199	1.0289
0.22354	1.7097
0.45495	1.895
0.94771	1.5853
1.4551	1.3234
1.476	1.3234
2.6796	0.92052
3.534	0.73804
4.1086	0.72881

Data for Figure 6

AA Conc.	Rate
0	0
0.55509	0.02138
1.6653	0.05780
2.7755	0.09351

Data for Figure 7

BP Conc.	Wt Gain
1	0.88002
5.03	1.0142
15.01	0.94939
30.05	0.94562

Data for Figure 8

AA Conc.	Wt Gain
0	0
5.05	5.77074
15	15.0245

Data for Figure 9

Wt Gain	PEG	Stdev	PP	Stdev	CA	Stdev
3.19	1369.4		1100		3.59.2	
3.73	1263.4		1100	100	3059.2	219.7
4.4	1271.2	61.3	1100		3059.2	
10.17	1046	15.7	1100			
1.82	1209.9	71.8	1100			
6.64	1111.2	128.8	1100			

Data for Figure 10

Pure Buffer Flux			
Time	PP	PEG	CA
Baseline	1100	1200	3100
Fouled Flux			
Time	PP	PEG	CA
0.34688	1222.3	1289.9	3034.9
0.68568	1094.7	1266.5	2132.3
1.0243	997.69	1184.6	1220.5
1.3604	949.9	1104	908.19
1.699	821.32	950.31	737.63
2.035	721.71	832.99	642.31
2.3737	650.21	747.61	568.61
2.7124	579.14	676.54	523.85
3.051	539.65	608.09	485.56
3.387	485.56	557.31	431.72
3.7257	434.35	515.96	421.88
4.0617	419.23	501.39	368.54
4.4003	392.31	458.22	361.77
4.7363	360.85	440.37	350.11
5.0742	329.82	408.97	329.01
5.4102	334.38	395.42	321.16
5.7488	308	363.27	297.18
6.0848	305.13	368.89	305.36
6.4235	281.67	350.11	289.21
6.7595	265.34	320.99	284.36
7.0982	273.77	310.63	260.61
7.4368	244.82	310.63	255.35
7.7755	242.18	313.26	265.33
8.1115	236.15	281.31	263.24
8.4502	231.65	281.67	236.15
8.7862	209.61	262.63	240.15
9.1249	229.02	257.98	228.19
9.46	207.48	262.73	239.55
9.7987	205.33	248.02	206.96
10.135	188.39	249.46	236.92

Time	PP	PEG	CA
10.473	205.33	236.92	212.27
10.809	188.39	241.41	207.96
11.148	179.01	202.7	212.27
11.487	176.37	233.54	207.96
11.825	186.94	215.05	189.54
12.161	156.55	209.57	205.33
12.5	184.27	209.66	188.39
12.836	161.85	205.33	186.94
13.175	155.31	193.66	204.31
13.511	169.81	202.7	184.7
13.849	166.26	191.08	167.16
14.185	145.93	184.27	179.04
14.523	155.31	183.05	196.35
14.859	159.2	184.34	168.48
15.198	134.25	185.7	175.12
15.534	156.55	166.23	163.21
15.873	136.89	188.42	186.9
16.211	157.95	157.95	168.48
16.55	134.25	183.12	156.55
16.886	137.98	163.21	152.68
17.225	128.99	161.82	159.2
17.561	140.63	127.3	165.85
17.899	128.99	143.28	156.54
18.235	138	134.25	168.9
18.573	131.92	137.98	145.94
18.909	111.44	134.26	151.32
19.248	139.55	138	163.12
19.584	124.7	137.2	135.4
19.922	118.46	140.63	160.49
20.258	130.01	134.28	137.98
20.597	118.46	111.44	155.34
20.936	102.66	134.26	139.52
21.274	128.99	137.98	139.52
21.61	114.09	110.56	137.97
21.946	111.44	134.25	136.89
22.285	113.19	110.56	135.32
22.621	92.867	132.67	147.42
22.96	115.83	115.83	127.36
23.296	108.79	122.05	137.23
23.634	110.84	128.99	135.32

Time	PP	PEG	CA
23.97	111.44	111.44	139.52
24.308	107.93	110.84	132.66
24.644	87.559	108.79	128.99
24.983	115.82	134.26	124.71
25.319	103.48	95.521	136.89
25.658	94.769	115.83	110.56
25.996	107.95	111.44	139.52
26.335	92.136	86.871	114.09
26.671	108.79	118.48	134.25
27.01	86.872	107.92	108.81
27.346	111.44	87.562	137.21
27.683	89.726	113.2	119.4
28.019	103.48	114.09	110.58
28.358	92.136	86.868	135.32
28.694	90.211	114.09	115.83
29.033	105.3	87.091	103.48
29.369	92.869	111.44	115.82
29.707	84.239	89.499	134.25
30.043	87.555	108.79	118.46
30.382	107.93	92.136	111.44
30.721	89.503	95.521	110.56
31.059	86.868	105.29	114.09
31.395	92.867	92.136	113.2
31.734	86.872	107.93	114.09
32.07	87.562	87.559	110.84
32.408	87.086	89.501	114.09
32.744	87.559	106.13	113.2
33.083	86.872	92.154	111.44
33.418	87.579	93.08	89.503
33.757	86.868	86.872	122.05
34.093	82.254	92.867	107.93
34.432	89.503	106.19	107.95
34.771	89.505	92.1	115.83
35.109	89.499	90.249	87.562
35.445	76.948	84.206	113.19
35.784	73.709	92.138	111.44
36.12	82.256	86.866	89.503
36.459	92.132	90.215	111.44
36.795	87.562	110.56	92.363
37.132	65.977	87.562	108.79

Time	PP	PEG	CA
37.468	84.903	94.764	105.3
37.807	92.136	87.562	100.83
38.143	61.028	79.172	107.93
38.482	89.503	92.863	90.213
38.818	82.25	92.138	97.402
39.156	65.812	82.254	100.03
39.495	89.505	71.076	92.134
39.834	84.251	90.215	114.09
40.17	68.988	89.499	89.503
40.508	84.239	81.608	90.215
40.844	66.334	97.415	110.58
41.183	86.87	82.256	90.213
41.519	66.331	92.136	87.073
41.857	87.091	92.867	111.44
42.193	63.68	57.915	89.523
42.532	84.235	92.863	87.562
42.868	63.682	87.091	90.249
43.206	65.812	87.562	113.15
43.542	87.559	86.866	90.213
43.881	63.178	68.988	84.239
44.22	81.606	81.606	89.505
44.558	68.445	87.562	89.499
44.894	63.68	65.809	90.215
45.233	84.235	94.769	92.136
45.569	68.988	89.503	84.908
45.905	63.68	68.988	113.48
46.243	63.335	86.868	92.867
46.579	79.649	84.908	84.239
46.917	71.034	68.445	82.256
47.253	66.334	84.924	94.764
47.592	68.455	89.706	84.908
47.928	61.028	66.347	78.973
48.267	65.812	92.136	79.602
48.603	63.68	63.67	89.516
48.941	68.445	89.499	84.239
49.28	63.176	61.04	92.138
49.619	57.915	92.136	87.555
49.955	66.334	65.809	86.872
50.293	63.176	92.136	90.215
50.629	68.988	63.668	89.724

Time	PP	PEG	CA
50.967	58.06	65.838	63.68
51.303	55.72	66.318	86.872
51.642	52.646	63.181	87.562
51.978	61.028	74.482	89.503
52.317	65.812	78.969	71.638
52.653	63.68	66.347	84.239
52.991	65.809	63.181	86.872
53.33	65.812	68.972	89.499
53.668	60.56	63.181	71.64
54.005	63.677	66.344	84.241
54.343	65.812	60.546	84.908
54.679	39.801	73.709	65.809
55.018	63.179	60.545	90.231
55.354	63.68	82.237	89.713
55.692	65.974	73.711	63.68
56.028	66.334	66.347	92.15
56.366	60.548	60.683	66.334
56.702	42.451	74.309	81.606
57.041	60.548	60.548	84.908
57.377	66.334	66.321	76.338
57.716	63.179	63.176	86.872
58.054	65.809	63.693	60.548
58.393	42.121	66.374	90.213
58.729	66.334	71.628	71.072
59.068	57.912	58.383	84.91
59.404	63.68	66.321	60.546
59.742	44.752	65.812	68.988
60.078	63.68	68.443	92.363
60.416	65.974	66.344	
Recovered Flux			
Time	PP	PEG	CA
	280	670	610

Data for Figure 11

Duration	Net flux	Stdev	Flux No BK		Stdev
0.1	146.6	3.2			
0.15	250	7.1			
0.2	242.5	15	120		7
0.3	223	7.3			
0.5	121.5	8.9			

Data for Figure 12

Duration	Net Flux	Stdev	Flux No Bk		Stdev
2	124.1	11.4			
4	242.5	15			
5	252	16.9	120		7
6	243.5	13.2			
8	191.6	16.3			

Data for Figure 13

Time	PEG	Time	AA	Time	DMA	Time	PP
0.58503	0.44	0.58952	0.67	1.1553	4.65	1.1553	4.82
1.1544	6.96	1.1617	5.82	1.7265	10.47	1.7255	9.15
1.7238	13.28	1.7292	10.5	2.2969	16.18	2.2932	12.44
2.294	18.34	2.3005	15.22	2.8672	21.29	2.8617	16.2
2.8617	23.44	2.8707	20.01	3.4357	25.8	3.432	19.5
3.4328	29.16	3.4383	24.58	4.0061	30.45	3.9995	22.65
4.0032	33.04	4.0095	28.99	4.5762	34.64	4.5698	25.72
4.5707	37.65	4.5798	33.48	5.1439	37.93	5.141	28.41
5.142	42.4	5.1502	37.77	5.715	42.3	5.7113	31.16
5.7124	46.36	5.7187	41.81	6.2854	45.48	6.2789	33.62
6.2825	50.55	6.289	45.61	6.8529	49.04	6.8501	35.99
6.851	56.12	6.8592	49.28	7.4242	52.6	7.4206	38.25
7.4214	58.67	7.4268	53	7.9945	56.01	7.9898	40.38
7.9917	62.64	7.998	56.54	8.562	59.06	8.5591	42.54
8.5639	66.54	8.5684	60.02	9.1332	62.48	9.1296	44.55
9.1332	70.37	9.1359	63.4	9.7046	65.29	9.6971	46.47
9.7035	74.11	9.7072	66.74	10.274	68.21	10.268	48.45
10.274	77.79	10.278	69.94	10.846	71.2	10.839	50.33
10.842	81.49	10.848	73.27	11.415	73.62	11.409	52.22

Time	PEG	Time	AA	Time	DMA	Time	PP
11.413	85.12	11.415	76.28	11.988	76.24	11.977	54.06
11.983	88.71	11.986	79.19	12.558	79.14	12.549	55.7
12.551	92.11	12.557	82.32	13.127	81.27	13.119	57.46
13.122	95.57	13.124	85.11	13.699	83.83	13.689	59.2
13.693	98.93	13.696	87.98	14.268	86.52	14.261	60.94
14.263	102.14	14.266	91.07	14.835	88.51	14.831	62.64
14.835	105.43	14.835	93.55	15.407	90.98	15.4	64.28
15.406	108.57	15.404	96.22	15.977	93.57	15.971	65.96
15.974	111.75	15.975	99.05	16.546	95.34	16.542	67.7
16.543	114.86	16.545	101.53	17.116	96.19	17.112	69.48
17.114	117.85	17.117	104.17	17.686	98.48	17.682	71.03
17.682	120.85	17.687	106.74	18.255	100.53	18.253	72.57
18.252	123.76	18.255	109.38	18.824	102.93	18.824	74.19
18.823	126.58	18.826	111.96	19.395	105.13	19.393	75.81
19.393	129.5	19.395	114.69	19.964	107.12	19.963	77.44
19.962	132.26	19.964	116.9	20.532	109.7	20.533	78.99
20.531	134.96	20.535	119.38	21.102	111.85	21.102	80.39
21.101	137.74	21.104	122.35	21.672	113.88	21.671	81.96
21.67	140.48	21.674	124.31	22.24	116	22.24	84.77
22.24	143.07	22.243	126.8	22.81	118.09	22.81	85.03
22.812	145.64	22.812	129.32	23.379	120.07	23.38	86.58
23.383	148.26	23.383	131.51	23.948	122.07	23.949	88.56
23.951	150.8	23.952	133.85	24.518	123.96	24.517	89.54
24.521	153.33	24.522	136.65	25.088	125.84	25.086	90.97
25.09	155.78	25.092	138.47	25.656	127.52	25.656	92.46
25.659	158.28	25.663	140.85	26.226	129.53	26.226	93.95
26.229	160.86	26.232	143.45	26.795	131.31	26.795	95.53
26.8	163.03	26.802	145.38	27.365	133.36	27.364	97.07
27.372	165.42	27.371	147.79	27.935	135.12	27.934	98.38
27.941	167.82	27.941	149.95	28.505	137.1	28.504	99.75
28.513	170.06	28.511	152.2	29.074	138.73	29.074	101.81
29.084	172.33	29.08	154.4	29.644	140.46	29.643	102.71
29.653	175.46	29.65	156.78	30.214	142.24	30.213	104.17
30.223	176.88	30.22	158.84	30.784	143.89	30.782	105.48
30.792	179.13	30.789	161.05	31.354	145.61	31.352	106.75
31.362	181.28	31.361	163.27	31.923	147.4	31.923	108.09
31.932	183.39	31.931	165.33	32.492	149	32.491	109.5
32.502	185.57	32.501	167.41	33.062	150.61	33.061	110.85
33.071	188.59	33.071	169.99	33.632	152.37	33.631	112.37
33.644	189.91	33.641	171.61	34.201	153.84	34.2	113.72

Time	PEG	Time	AA	Time	DMA	Time	PP
34.214	191.85	34.208	173.7	34.773	155.62	34.771	114.97
34.784	194.43	34.78	175.93	35.342	157.33	35.342	116.45
35.355	196.01	35.349	177.72	35.91	158.91	35.912	118.55
35.923	197.96	35.919	179.85	36.48	160.56	36.482	118.97
36.493	200.26	36.49	182.43	37.05	162.18	37.053	120.42
37.064	201.95	37.061	183.85	37.62	163.8	37.624	121.72
37.634	203.97	37.629	185.79	38.189	165.4	38.193	123.13
38.206	205.88	38.2	188	38.759	166.9	38.762	124.45
38.776	207.76	38.77	189.75	39.329	168.3	39.333	125.74
39.345	209.7	39.339	191.64	39.898	169.85	39.903	126.97
39.915	211.58	39.908	194.18	40.468	171.37	40.474	128.39
40.485	213.46	40.479	195.55	41.039	172.99	41.044	129.67
41.058	215.21	41.049	197.34	41.608	174.48	41.612	130.98
41.628	217.18	41.621	199.06	42.178	176.02	42.183	132.26
42.198	219.06	42.19	200.86	42.748	177.63	42.753	133.59
42.77	220.65	42.76	202.48	43.317	179.28	43.323	134.78
43.341	222.45	43.33	204.29	43.887	180.78	43.895	136.21
43.91	224.16	43.899	206.01	44.456	182.45	44.466	137.35
44.48	225.74	44.468	207.65	45.026	184.08	45.036	138.62
45.05	227.42	45.039	209.25	45.597	185.49	45.607	139.94
45.618	229.03	45.608	210.85	46.164	186.82	46.179	141.19
46.188	230.69	46.177	212.62	46.735	188.48	46.748	142.47
46.758	232.28	46.747	214.23	47.307	190	47.319	143.65
47.328	234.01	47.317	215.99	47.875	191.49	47.89	144.94
47.897	235.48	47.888	217.61	48.446	193.07	48.46	146.48
48.465	237.14	48.458	219.23	49.017	194.49	49.03	147.47
49.034	238.7	49.026	220.91	49.587	195.9	49.601	148.71
49.603	240.3	49.598	222.42	50.155	197.47	50.168	149.98
50.172	241.89	50.168	224.22	50.727	198.7	50.739	151.03
50.743	243.48	50.74	225.67	51.297	199.52	51.31	152.4
51.312	244.9	51.311	227.3	51.865	201.17	51.88	154.06
51.882	246.63	51.88	228.86	52.437	202.41	52.452	154.83
52.452	248.02	52.448	230.42	53.007	204.05	53.021	156.05
53.021	249.46	53.018	231.92	53.574	205.53	53.593	157.23
53.591	250.9	53.589	233.38	54.143	206.91	54.163	158.5
54.161	252.34	54.159	234.94	54.713	208.33	54.734	159.64
54.729	253.8	54.729	236.42	55.281	209.66	55.305	160.7
55.3	255.23	55.299	237.9	55.851	211.02	55.875	161.85
55.869	256.59	55.869	239.38	56.423	212.5	56.442	163.08
56.437	258.05	56.439	240.86	56.993	213.88	57.014	164.3

Time	PEG	Time	AA	Time	DMA	Time	PP
57.006	259.56	57.009	242.34	57.56	215.18	57.584	165.3
57.575	260.96	57.579	243.82	58.131	216.54	58.152	166.61
58.143	262.38	58.149	245.3	58.702	217.76	58.723	167.75
58.713	264	58.719	246.78	59.269	218.99	59.293	168.83
		59.289	248.26	59.841	220.46	59.861	169.95
		59.859	249.74				
Time	PP No BK		PEG No BK		CA		CA No BK
0.34688	4.63	0.34779	4.9	0.01914	0	0.34798	11.5
0.68568	8.79	0.68568	9.7	0.59134	10.01	0.68665	19.6
1.0243	12.58	1.0243	14.2	1.1625	21.74	1.0227	24.2
1.3604	16.16	1.3603	18.36	1.7301	31.64	1.3613	27.65
1.699	19.28	1.699	21.97	2.3013	40.43	1.6973	30.43
2.035	22	2.035	25.11	2.8716	48.27	2.036	32.87
2.3737	24.47	2.3737	27.95	3.4391	55.48	2.3747	35.03
2.7124	26.67	2.7124	30.52	4.0105	61.85	2.7133	37.02
3.051	28.72	3.051	32.83	4.5807	68.11	3.0493	38.85
3.387	30.55	3.387	34.93	5.151	74.1	3.388	40.49
3.7257	32.2	3.7257	36.89	5.7195	79.68	3.724	42.08
4.0617	33.78	4.0617	38.78	6.2898	85.18	4.0627	43.48
4.4003	35.27	4.4003	40.52	6.861	90.19	4.3979	44.84
4.7363	36.63	4.7363	42.18	7.4313	95.06	4.7365	46.17
5.0742	37.88	5.0742	43.73	8.0016	99.89	5.0725	47.41
5.4102	39.14	5.4102	45.22	8.572	104.14	5.4112	48.63
5.7488	40.31	5.7488	46.6	9.1395	108.43	5.7472	49.75
6.0848	41.46	6.0848	47.99	9.7108	113.3	6.0859	50.91
6.4235	42.53	6.4234	49.32	10.281	116.49	6.4219	52
6.7595	43.53	6.7595	50.53	10.852	120.37	6.7605	53.08
7.0982	44.57	7.0982	51.71	11.422	124.7	7.0992	54.07
7.4368	45.5	7.4368	52.89	11.993	127.5	7.4378	55.04
7.7755	46.42	7.7755	54.08	12.565	130.96	7.7738	56.04
8.1115	47.31	8.1115	55.14	13.136	134.37	8.1125	57.04
8.4502	48.19	8.4501	56.21	13.707	137.66	8.4485	57.93
8.7862	48.98	8.7862	57.2	14.278	140.93	8.7863	58.84
9.1249	49.85	9.1249	58.18	14.848	143.98	9.1223	59.7
9.46	50.63	9.4608	59.17	15.416	147.02	9.461	60.61
9.7987	51.41	9.7987	60.11	15.986	150.01	9.797	61.39
10.135	52.12	10.135	61.05	16.557	152.9	10.136	62.29
10.473	52.9	10.473	61.95	17.127	155.66	10.472	63.09

Time	PP No BK		PEG No BK		CA		CA No BK
10.809	53.61	10.809	62.86	17.697	158.34	10.81	63.88
11.148	54.29	11:148	63.63	18.267	160.9	11.146	64.68
11.487	54.96	11.484	64.51	18.837	163.48	11.485	65.47
11.825	55.67	11.82	65.32	19.407	166.01	11.824	66.19
12.161	56.26	12.156	66.11	19.975	168.51	12.162	66.97
12.5	56.96	12.492	66.9	20.545	170.92	12.498	67.68
12.836	57.57	12.83	67.68	21.114	173.23	12.837	68.39
13.175	58.16	13.167	68.41	21.684	175.5	13.173	69.16
13.511	58.8	13.505	69.18	22.253	177.75	13.511	69.86
13.849	59.43	13.841	69.9	22.821	179.95	13.847	70.49
14.185	59.98	14.18	70.6	23.391	182.07	14.185	71.17
14.523	60.57	14.516	71.29	23.96	184.12	14.521	71.91
14.859	61.17	14.854	71.99	24.532	186.24	14.86	72.55
15.198	61.68	15.19	72.69	25.1	188.25	15.196	73.21
15.534	62.27	15.528	73.32	25.669	190.22	15.535	73.83
15.873	62.79	15.864	74.03	26.239	192.26	15.874	74.54
16.211	63.39	16.203	74.63	26.809	194.16	16.212	75.18
16.55	63.9	16.539	75.32	27.378	196.05	16.548	75.77
16.886	64.42	16.878	75.94	27.95	197.8	16.887	76.35
17.225	64.91	17.214	76.55	28.517	199.69	17.223	76.95
17.561	65.44	17.557	77.04	29.088	201.49	17.562	77.58
17.899	65.93	17.893	77.58	29.657	203.23	17.898	78.17
18.235	66.45	18.232	78.09	30.227	204.87	18.235	78.81
18.573	66.95	18.568	78.61	30.797	206.66	18.571	79.36
18.909	67.37	18.906	79.12	31.367	208.23	18.907	79.93
19.248	67.9	19.242	79.64	31.935	209.83	19.246	80.55
19.584	68.37	19.58	80.16	32.505	211.64	19.582	81.06
19.922	68.82	19.916	80.69	33.075	213.63	19.921	81.67
20.258	69.31	20.255	81.2	33.644	215.62	20.257	82.19
20.597	69.76	20.591	81.62	34.214	217.74	20.595	82.78
20.936	70.15	20.929	82.13	34.785	219.75	20.934	83.31
21.274	70.64	21.265	82.65	35.354	221.68	21.273	83.84
21.61	71.07	21.604	83.07	35.923	223.56	21.609	84.36
21.946	71.49	21.943	83.58	36.493	225.29	21.947	84.88
22.285	71.92	22.281	84	37.063	227.04	22.283	85.39
22.621	72.27	22.617	84.5	37.632	228.34	22.622	85.95
22.96	72.71	22.956	84.94	38.205	229.81	22.958	86.43
23.296	73.12	23.292	85.4	38.775	231.31	23.296	86.95
23.634	73.54	23.631	85.89	39.344	232.7	23.632	87.46

Time	PP No BK		PEG No BK		CA		CA No BK
23.97	73.96	23.967	86.31	39.913	234.04	23.971	87.99
24.308	74.37	24.305	86.73	40.484	235.31	24.307	88.49
24.644	74.7	24.64	87.14	41.053	236.55	24.645	88.98
24.983	75.14	24.979	87.65	41.624	237.84	24.981	89.45
25.319	75.53	25.315	88.01	42.193	239.02	25.32	89.97
25.658	75.89	25.654	88.45	42.763	240.18	25.659	90.39
25.996	76.3	25.99	88.87	43.331	241.25	25.997	90.92
26.335	76.65	26.329	89.2	43.901	242.41	26.333	91.35
26.671	77.06	26.667	89.65	44.472	243.44	26.672	91.86
27.01	77.39	27.006	90.06	45.042	244.51	27.008	92.27
27.346	77.81	27.342	90.39	45.613	245.58	27.346	92.79
27.683	78.15	27.68	90.82	46.183	246.28	27.682	93.24
28.019	78.54	28.016	91.25	46.752	247.04	28.02	93.66
28.358	78.89	28.355	91.58	47.32	247.74	28.356	94.17
28.694	79.23	28.691	92.01	47.891	248.52	28.695	94.61
29.033	79.63	29.029	92.34	48.462	249.26	29.031	95
29.369	79.98	29.365	92.76	49.029	250	29.37	95.44
29.707	80.3	29.704	93.1	49.6	250.92	29.708	95.95
30.043	80.63	30.04	93.51	50.171	251.66	30.047	96.4
30.382	81.04	30.378	93.86	50.741	252.41	30.383	96.82
30.721	81.38	30.714	94.22	51.311	253.2	30.722	97.24
31.059	81.71	31.053	94.62	51.883	253.91	31.058	97.67
31.395	82.06	31.392	94.97	52.453	254.62	31.396	98.1
31.734	82.39	31.73	95.38	53.023	255.43	31.732	98.53
32.07	82.72	32.066	95.71	53.594	256.18	32.07	98.95
32.408	83.05	32.405	96.05	54.166	256.83	32.406	99.38
32.744	83.38	32.741	96.45	54.736	258.14	32.745	99.81
33.083	83.71	33.08	96.8	55.305	258.28	33.081	100.23
33.418	84.04	33.415	97.15	55.875	259.02	33.42	100.57
33.757	84.37	33.754	97.48	56.445	259.86	33.756	101.03
34.093	84.68	34.09	97.83	57.015	260.48	34.094	101.44
34.432	85.02	34.425	98.23	57.586	261.18	34.433	101.85
34.771	85.36	34.764	98.58	58.157	263.04	34.771	102.29
35.109	85.7	35.1	98.92	58.727	262.5	35.107	102.62
35.445	85.99	35.439	99.24	59.296	263.3	35.446	103.05
35.784	86.27	35.777	99.59	59.866	264.36	35.782	103.47
36.12	86.58	36.116	99.92	60.435	264.65	36.121	103.81
36.459	86.93	36.452	100.26			36.457	104.23
36.795	87.26	36.791	100.68			36.795	104.58

Time	PP No BK		PEG No BK		CA		CA No BK
37.132	87.51	37.127	101.01			37.131	104.99
37.468	87.83	37.465	101.37			37.469	105.39
37.807	88.18	37.801	101.7			37.805	105.77
38.143	88.41	38.139	102			38.144	106.18
38.482	88.75	38.475	102.35			38.48	106.52
38.818	89.06	38.814	102.7			38.819	106.89
39.156	89.31	39.15	103.01			39.157	107.27
39.495	89.65	39.489	103.28			39.496	107.62
39.834	89.97	39.825	103.62			39.832	108.05
40.17	90.23	40.163	103.96			40.171	108.39
40.508	90.55	40.502	104.27			40.507	108.73
40.844	90.8	40.841	104.64			40.845	109.15
41.183	91.13	41.177	104.95			41.181	109.49
41.519	91.38	41.515	105.3			41.519	109.82
41.857	91.71	41.851	105.65			41.855	110.24
42.193	91.95	42.19	105.87			42.194	110.58
42.532	92.27	42.526	106.22			42.53	110.91
42.868	92.51	42.864	106.55			42.866	111.25
43.206	92.76	43.2	106.88			43.204	111.68
43.542	93.09	43.538	107.21			43.541	112.02
43.881	93.33	43.874	107.47			43.879	112.34
44.22	93.64	44.213	107.78			44.218	112.68
44.558	93.9	44.549	108.11			44.557	113.02
44.894	94.14	44.888	108.36			44.893	113.36
45.233	94.46	45.227	108.72			45.231	113.71
45.569	94.72	45.565	109.06			45.567	114.03
45.905	94.96	45.901	109.32			45.905	114.46
46.243	95.2	46.24	109.65			46.241	114.81
46.579	95.5	46.576	109.97			46.58	115.13
46.917	95.77	46.915	110.23			46.916	115.44
47.253	96.02	47.25	110.55			47.254	115.8
47.592	96.28	47.588	110.89			47.59	116.12
47.928	96.51	47.924	111.14			47.929	116.42
48.267	96.76	48.263	111.49			48.265	116.72
48.603	97	48.599	111.73			48.604	117.06
48.941	97.26	48.938	112.07			48.942	117.38
49.28	97.5	49.274	112.3			49.281	117.73
49.619	97.72	49.612	112.65			49.617	118.06
49.955	97.97	49.951	112.9			49.956	118.39

Time	PP No BK		PEG No BK		CA		CA No BK
50.293	98.21	50.29	113.25			50.292	118.73
50.629	98.47	50.626	113.49			50.63	119.07
50.967	98.69	50.964	113.74			50.965	119.31
51.303	98.9	51.3	113.99			51.304	119.64
51.642	99.1	51.639	114.23			51.64	119.97
51.978	99.33	51.974	114.51			51.979	120.31
52.317	99.58	52.313	114.81			52.315	120.58
52.653	99.82	52.649	115.06			52.654	120.9
52.991	100.07	52.987	115.3			52.992	121.23
53.33	100.32	53.324	115.56			53.331	121.57
53.668	100.55	53.662	115.8			53.667	121.84
54.005	100.79	53.998	116.05			54.006	122.16
54.343	101.04	54.337	116.28			54.342	122.48
54.679	101.19	54.675	116.56			54.68	122.73
55.018	101.43	55.014	116.79			55.016	123.07
55.354	101.67	55.35	117.1			55.354	123.41
55.692	101.92	55.689	117.38			55.69	123.65
56.028	102.17	56.025	117.63			56.029	124
56.366	102.4	56.363	117.86			56.365	124.25
56.702	102.56	56.699	118.14			56.703	124.56
57.041	102.79	57.037	118.37			57.039	124.88
57.377	103.04	57.373	118.62			57.378	125.17
57.716	103.28	57.712	118.86			57.717	125.5
58.054	103.53	58.048	119.1			58.055	125.73
58.393	103.69	58.384	119.35			58.391	126.07
58.729	103.94	58.72	119.62			58.73	126.34
59.068	104.16	59.056	119.84			59.066	126.66
59.404	104.4	59.392	120.09			59.405	126.89
59.742	104.57	59.731	120.34			59.741	127.15
/60.078	104.81	60.069	120.6			60.079	127.5
60.416	105.06	60.405	120.85				

Data for Figure 14

Wt Gain	Long-term Flux		Recovered Flux	
4.88	168		363.2	
3.19	153.6		295.6	
3.73	154.4		315.8	
10.42	173.6		401.8	
10.13	148		326.5	
9.96	134.4		335.2	
6.64	121.6		386.4	
6.64	115.2		301.2	
0	128		210	
1.81	181			
1.83	139		323.4	